Code-Verification Techniques for Hypersonic Reacting Flows in Thermochemical Nonequilibrium

Brian A. Freno
Brian R. Carnes
V. Gregory Weirs
Sandia National Laboratories

ASME Verification & Validation Symposium
May 19–20, 2021

Outline

- Introduction
- Governing Equations
- Verification Techniques for Spatial Accuracy
- Spatial-Discretization Verification Results
- Verification Techniques for Thermochemical Source Term
- Thermochemical-Source-Term Verification Results
- Summary

Outline

- Introduction
  - Hypersonic Flow
  - Sandia Parallel Aerodynamics and Reentry Code (`SPARC`)
  - Verification and Validation
- Governing Equations
- Verification Techniques for Spatial Accuracy
- Spatial-Discretization Verification Results
- Verification Techniques for Thermochemical Source Term
- Thermochemical-Source-Term Verification Results
- Summary

Hypersonic Flow

Hypersonic flows and underlying aerothermochemical phenomena

- Important in design & analysis of vehicles exiting/reentering atmosphere
- High flow velocities and stagnation enthalpies
  - Induce chemical reactions
  - Excite thermal energy modes
- Aerodynamic and thermochemical models require full coupling

Sandia Parallel Aerodynamics and Reentry Code (SPARC)

Sandia Parallel Aerodynamics and Reentry Code (SPARC)

- Under development at Sandia National Laboratories
- Compressible computational fluids dynamics code
- Models transonic and hypersonic reacting turbulent flows
- Solves transient heat equation and equations associated with decomposing and non-decomposing ablators
- One- and two-way couplings between fluid-dynamics and ablation solvers

Verification and Validation

Credibility of computational physics codes requires verification and validation

- **Validation** assesses how well models represent physical phenomena
  - Computational results are compared with experimental results
  - Assess suitability of models, model error, and bounds of validity

- **Verification** assesses accuracy of numerical solutions against expectations
  - *Solution verification* estimates numerical error for particular solution
  - *Code verification* verifies correctness of numerical-method implementation

Code Verification

Code verification is focus of this work

- Governing equations are numerically discretized
  - Discretization error is introduced in solution
- Seek to verify discretization error decreases with refinement of discretization
  - Should decrease at an expected rate
- Use manufactured and exact solutions to compute error

Code Verification

Code verification demonstrated in many computational physics disciplines

- Fluid dynamics
- Solid mechanics
- Heat transfer
- Multiphase flows
- Electrodynamics
- Electromagnetism
- Fluid–structure interaction
- Radiation hydrodynamics

Code-verification techniques for hypersonic flows have been presented

- Single-species perfect gas
- Multi-species gas in thermal equilibrium

We present code-verification techniques for hypersonic reacting flows in thermochemical **nonequilibrium** and demonstrate effectiveness

- Spatial discretization
- Thermochemical source term

Outline

- Introduction
- Governing Equations
  - Conserved Quantities
  - Vibrational Energy
  - Translational–Vibrational Energy Exchange
  - Chemical Kinetics
  - Scope of Code Verification
- Verification Techniques for Spatial Accuracy
- Spatial-Discretization Verification Results
- Verification Techniques for Thermochemical Source Term
- Thermochemical-Source-Term Verification Results
- Summary

Governing Equations: n_s Species in Vibrational Nonequilibrium

Conservation of mass, momentum, and energy:

$$\frac{\partial \mathbf{U}}{\partial t} + \nabla \cdot \mathbf{F}_c(\mathbf{U}) = -\nabla \cdot \mathbf{F}_p(\mathbf{U}) + \nabla \cdot \mathbf{F}_d(\mathbf{U}) + \mathbf{S}(\mathbf{U}),$$

where

$$\mathbf{U} = \begin{Bmatrix} \boldsymbol{\rho} \\ \rho\mathbf{v} \\ \rho E \\ \rho e_v \end{Bmatrix}, \quad \mathbf{F}_c(\mathbf{U}) = \begin{bmatrix} \boldsymbol{\rho}\mathbf{v}^T \\ \rho\mathbf{v}\mathbf{v}^T \\ \rho E\mathbf{v}^T \\ \rho e_v\mathbf{v}^T \end{bmatrix}, \quad \mathbf{F}_p(\mathbf{U}) = \begin{bmatrix} \mathbf{0} \\ p\mathbf{I} \\ p\mathbf{v}^T \\ \mathbf{0}^T \end{bmatrix}, \quad \mathbf{F}_d(\mathbf{U}) = \begin{bmatrix} -\mathbf{J} \\ \boldsymbol{\tau} \\ \left(\boldsymbol{\tau}\mathbf{v} - \mathbf{q} - \mathbf{q}_v - \mathbf{J}^T\mathbf{h}\right)^T \\ \left(-\mathbf{q}_v - \mathbf{J}^T\mathbf{e}_v\right)^T \end{bmatrix},$$

$$\mathbf{S}(\mathbf{U}) = \begin{Bmatrix} \dot{\mathbf{w}} \\ \mathbf{0} \\ 0 \\ Q_{t-v} + \mathbf{e}_v^T\dot{\mathbf{w}} \end{Bmatrix},$$

$$\boldsymbol{\rho} = \{\rho_1, \dots, \rho_{n_s}\}^T, \qquad \rho = \sum_{s=1}^{n_s} \rho_s, \qquad p = \sum_{s=1}^{n_s} \frac{\rho_s}{M_s}\bar{R}T,$$

$\dot{\mathbf{w}} = \{\dot{w}_1, \dots, \dot{w}_{n_s}\}^T$: mass production rates per volume,

$e_v = \sum_{s=1}^{n_s} \frac{\rho_s}{\rho} e_{v_s}$: mixture vibrational energy per mass,

$\mathbf{e}_v = \left\{e_{v_1}, \dots, e_{v_{n_s}}\right\}^T$: vibrational energies per mass,

Q_{t-v} : translational–vibrational energy exchange,

$$E = \frac{|\mathbf{v}|^2}{2} + \sum_{s=1}^{n_s} \frac{\rho_s}{\rho}\left(c_{\mathcal{V}_s}T + e_{v_s} + h_s^o\right)$$

Governing Equations: n_s Species in Vibrational Nonequilibrium

Conservation of mass, momentum, and energy:

$$\frac{\partial \mathbf{U}}{\partial t} + \nabla \cdot \mathbf{F}_c(\mathbf{U}) = -\nabla \cdot \mathbf{F}_p(\mathbf{U}) + \nabla \cdot \mathbf{F}_d(\mathbf{U}) + \mathbf{S}(\mathbf{U}),$$

where

$$\mathbf{U} = \begin{Bmatrix} \boldsymbol{\rho} \\ \rho\mathbf{v} \\ \rho E \\ \rho e_v \end{Bmatrix}, \quad \mathbf{F}_c(\mathbf{U}) = \begin{bmatrix} \boldsymbol{\rho}\mathbf{v}^T \\ \rho\mathbf{v}\mathbf{v}^T \\ \rho E\mathbf{v}^T \\ \rho e_v \mathbf{v}^T \end{bmatrix}, \quad \mathbf{F}_p(\mathbf{U}) = \begin{bmatrix} \mathbf{0} \\ p\mathbf{I} \\ p\mathbf{v}^T \\ \mathbf{0}^T \end{bmatrix}, \quad \mathbf{F}_d(\mathbf{U}) = \begin{bmatrix} -\mathbf{J} \\ \boldsymbol{\tau} \\ \left(\boldsymbol{\tau}\mathbf{v} - \mathbf{q} - \mathbf{q}_v - \mathbf{J}^T\mathbf{h}\right)^T \\ \left(-\mathbf{q}_v - \mathbf{J}^T\mathbf{e}_v\right)^T \end{bmatrix},$$

$$\mathbf{S}(\mathbf{U}) = \begin{Bmatrix} \dot{\mathbf{w}} \\ \mathbf{0} \\ 0 \\ Q_{t-v} + \mathbf{e}_v^T\dot{\mathbf{w}} \end{Bmatrix},$$

Multiple species

$\boldsymbol{\rho} = \{\rho_1, \dots, \rho_{n_s}\}^T$, $\quad \dot{\mathbf{w}} = \{\dot{w}_1, \dots, \dot{w}_{n_s}\}^T$: mass production rates per volume,

$\rho = \sum_{s=1}^{n_s} \rho_s$, $\quad e_v = \sum_{s=1}^{n_s} \frac{\rho_s}{\rho} e_{v_s}$: mixture vibrational energy per mass,

$p = \sum_{s=1}^{n_s} \frac{\rho_s}{M_s} \bar{R} T$, $\quad \mathbf{e}_v = \{e_{v_1}, \dots, e_{v_{n_s}}\}^T$: vibrational energies per mass,

Q_{t-v}: translational–vibrational energy exchange,

$$E = \frac{|\mathbf{v}|^2}{2} + \sum_{s=1}^{n_s} \frac{\rho_s}{\rho}\left(c_{\mathcal{V}_s} T + e_{v_s} + h_s^o\right)$$

Governing Equations: n_s Species in Vibrational Nonequilibrium

Conservation of mass, momentum, and energy:

Local time derivative

$$\frac{\partial \mathbf{U}}{\partial t} + \nabla \cdot \mathbf{F}_c(\mathbf{U}) = -\nabla \cdot \mathbf{F}_p(\mathbf{U}) + \nabla \cdot \mathbf{F}_d(\mathbf{U}) + \mathbf{S}(\mathbf{U}),$$

where

$$\mathbf{U} = \begin{Bmatrix} \boldsymbol{\rho} \\ \rho\mathbf{v} \\ \rho E \\ \rho e_v \end{Bmatrix}, \quad \mathbf{F}_c(\mathbf{U}) = \begin{bmatrix} \boldsymbol{\rho}\mathbf{v}^T \\ \rho\mathbf{v}\mathbf{v}^T \\ \rho E\mathbf{v}^T \\ \rho e_v\mathbf{v}^T \end{bmatrix}, \quad \mathbf{F}_p(\mathbf{U}) = \begin{bmatrix} \mathbf{0} \\ p\mathbf{I} \\ p\mathbf{v}^T \\ \mathbf{0}^T \end{bmatrix}, \quad \mathbf{F}_d(\mathbf{U}) = \begin{bmatrix} -\mathbf{J} \\ \boldsymbol{\tau} \\ \left(\boldsymbol{\tau}\mathbf{v} - \mathbf{q} - \mathbf{q}_v - \mathbf{J}^T\mathbf{h}\right)^T \\ \left(-\mathbf{q}_v - \mathbf{J}^T\mathbf{e}_v\right)^T \end{bmatrix},$$

$$\mathbf{S}(\mathbf{U}) = \begin{Bmatrix} \dot{\mathbf{w}} \\ \mathbf{0} \\ 0 \\ Q_{t-v} + \mathbf{e}_v^T\dot{\mathbf{w}} \end{Bmatrix},$$

$\boldsymbol{\rho} = \{\rho_1, \dots, \rho_{n_s}\}^T$, $\quad \dot{\mathbf{w}} = \{\dot{w}_1, \dots, \dot{w}_{n_s}\}^T$: mass production rates per volume,

$\rho = \sum_{s=1}^{n_s} \rho_s$, $\quad e_v = \sum_{s=1}^{n_s} \frac{\rho_s}{\rho} e_{v_s}$: mixture vibrational energy per mass,

$p = \sum_{s=1}^{n_s} \frac{\rho_s}{M_s} \bar{R} T$, $\quad \mathbf{e}_v = \{e_{v_1}, \dots, e_{v_{n_s}}\}^T$: vibrational energies per mass,

Q_{t-v} : translational–vibrational energy exchange,

$$E = \frac{|\mathbf{v}|^2}{2} + \sum_{s=1}^{n_s} \frac{\rho_s}{\rho}\left(c_{\mathcal{V}_s} T + e_{v_s} + h_s^o\right)$$

Governing Equations: n_s Species in Vibrational Nonequilibrium

Conservation of mass, momentum, and energy:

Convective flux gradient

$$\frac{\partial \mathbf{U}}{\partial t} + \nabla \cdot \mathbf{F}_c(\mathbf{U}) = -\nabla \cdot \mathbf{F}_p(\mathbf{U}) + \nabla \cdot \mathbf{F}_d(\mathbf{U}) + \mathbf{S}(\mathbf{U}),$$

where

$$\mathbf{U} = \begin{Bmatrix} \boldsymbol{\rho} \\ \rho\mathbf{v} \\ \rho E \\ \rho e_v \end{Bmatrix}, \quad \mathbf{F}_c(\mathbf{U}) = \begin{bmatrix} \boldsymbol{\rho}\mathbf{v}^T \\ \rho\mathbf{v}\mathbf{v}^T \\ \rho E\mathbf{v}^T \\ \rho e_v\mathbf{v}^T \end{bmatrix}, \quad \mathbf{F}_p(\mathbf{U}) = \begin{bmatrix} \mathbf{0} \\ p\mathbf{I} \\ p\mathbf{v}^T \\ \mathbf{0}^T \end{bmatrix}, \quad \mathbf{F}_d(\mathbf{U}) = \begin{bmatrix} -\mathbf{J} \\ \boldsymbol{\tau} \\ \left(\boldsymbol{\tau}\mathbf{v} - \mathbf{q} - \mathbf{q}_v - \mathbf{J}^T\mathbf{h}\right)^T \\ \left(-\mathbf{q}_v - \mathbf{J}^T\mathbf{e}_v\right)^T \end{bmatrix},$$

$$\mathbf{S}(\mathbf{U}) = \begin{Bmatrix} \dot{\mathbf{w}} \\ \mathbf{0} \\ 0 \\ Q_{t-v} + \mathbf{e}_v^T\dot{\mathbf{w}} \end{Bmatrix},$$

$\boldsymbol{\rho} = \{\rho_1, \dots, \rho_{n_s}\}^T$, $\quad \dot{\mathbf{w}} = \{\dot{w}_1, \dots, \dot{w}_{n_s}\}^T$: mass production rates per volume,

$\rho = \sum_{s=1}^{n_s} \rho_s$, $\quad e_v = \sum_{s=1}^{n_s} \frac{\rho_s}{\rho} e_{v_s}$: mixture vibrational energy per mass,

$p = \sum_{s=1}^{n_s} \frac{\rho_s}{M_s} \bar{R}T$, $\quad \mathbf{e}_v = \{e_{v_1}, \dots, e_{v_{n_s}}\}^T$: vibrational energies per mass,

Q_{t-v}: translational–vibrational energy exchange,

$$E = \frac{|\mathbf{v}|^2}{2} + \sum_{s=1}^{n_s} \frac{\rho_s}{\rho}\left(c_{\mathcal{V}_s}T + e_{v_s} + h_s^o\right)$$

Governing Equations: n_s Species in Vibrational Nonequilibrium

Conservation of mass, momentum, and energy:

$$\frac{\partial \mathbf{U}}{\partial t} + \nabla \cdot \mathbf{F}_c(\mathbf{U}) = \underbrace{-\nabla \cdot \mathbf{F}_p(\mathbf{U})}_{\text{Pressure flux gradient}} + \nabla \cdot \mathbf{F}_d(\mathbf{U}) + \mathbf{S}(\mathbf{U}),$$

where

$$\mathbf{U} = \begin{Bmatrix} \boldsymbol{\rho} \\ \rho\mathbf{v} \\ \rho E \\ \rho e_v \end{Bmatrix}, \quad \mathbf{F}_c(\mathbf{U}) = \begin{bmatrix} \boldsymbol{\rho}\mathbf{v}^T \\ \rho\mathbf{v}\mathbf{v}^T \\ \rho E\mathbf{v}^T \\ \rho e_v\mathbf{v}^T \end{bmatrix}, \quad \mathbf{F}_p(\mathbf{U}) = \begin{bmatrix} \mathbf{0} \\ p\mathbf{I} \\ p\mathbf{v}^T \\ \mathbf{0}^T \end{bmatrix}, \quad \mathbf{F}_d(\mathbf{U}) = \begin{bmatrix} -\mathbf{J} \\ \boldsymbol{\tau} \\ \left(\boldsymbol{\tau}\mathbf{v} - \mathbf{q} - \mathbf{q}_v - \mathbf{J}^T\mathbf{h}\right)^T \\ \left(-\mathbf{q}_v - \mathbf{J}^T\mathbf{e}_v\right)^T \end{bmatrix},$$

$$\mathbf{S}(\mathbf{U}) = \begin{Bmatrix} \dot{\mathbf{w}} \\ \mathbf{0} \\ 0 \\ Q_{t-v} + \mathbf{e}_v^T\dot{\mathbf{w}} \end{Bmatrix},$$

$\boldsymbol{\rho} = \{\rho_1, \dots, \rho_{n_s}\}^T$, $\quad \dot{\mathbf{w}} = \{\dot{w}_1, \dots, \dot{w}_{n_s}\}^T$: mass production rates per volume,

$\rho = \sum_{s=1}^{n_s} \rho_s$, $\quad e_v = \sum_{s=1}^{n_s} \frac{\rho_s}{\rho} e_{v_s}$: mixture vibrational energy per mass,

$p = \sum_{s=1}^{n_s} \frac{\rho_s}{M_s} \bar{R} T$, $\quad \mathbf{e}_v = \{e_{v_1}, \dots, e_{v_{n_s}}\}^T$: vibrational energies per mass,

Q_{t-v}: translational–vibrational energy exchange,

$$E = \frac{|\mathbf{v}|^2}{2} + \sum_{s=1}^{n_s} \frac{\rho_s}{\rho} \left(c_{\mathcal{V}_s} T + e_{v_s} + h_s^o\right)$$

Governing Equations: n_s Species in Vibrational Nonequilibrium

Conservation of mass, momentum, and energy:

Diffusive flux gradient

$$\frac{\partial \mathbf{U}}{\partial t} + \nabla \cdot \mathbf{F}_c(\mathbf{U}) = -\nabla \cdot \mathbf{F}_p(\mathbf{U}) + \nabla \cdot \mathbf{F}_d(\mathbf{U}) + \mathbf{S}(\mathbf{U}),$$

where

$$\mathbf{U} = \begin{Bmatrix} \boldsymbol{\rho} \\ \rho\mathbf{v} \\ \rho E \\ \rho e_v \end{Bmatrix}, \quad \mathbf{F}_c(\mathbf{U}) = \begin{bmatrix} \boldsymbol{\rho}\mathbf{v}^T \\ \rho\mathbf{v}\mathbf{v}^T \\ \rho E\mathbf{v}^T \\ \rho e_v\mathbf{v}^T \end{bmatrix}, \quad \mathbf{F}_p(\mathbf{U}) = \begin{bmatrix} \mathbf{0} \\ p\mathbf{I} \\ p\mathbf{v}^T \\ \mathbf{0}^T \end{bmatrix}, \quad \mathbf{F}_d(\mathbf{U}) = \begin{bmatrix} -\mathbf{J} \\ \boldsymbol{\tau} \\ \left(\boldsymbol{\tau}\mathbf{v} - \mathbf{q} - \mathbf{q}_v - \mathbf{J}^T\mathbf{h}\right)^T \\ \left(-\mathbf{q}_v - \mathbf{J}^T\mathbf{e}_v\right)^T \end{bmatrix},$$

$$\mathbf{S}(\mathbf{U}) = \begin{Bmatrix} \dot{\mathbf{w}} \\ \mathbf{0} \\ 0 \\ Q_{t-v} + \mathbf{e}_v^T\dot{\mathbf{w}} \end{Bmatrix},$$

$\boldsymbol{\rho} = \{\rho_1, \dots, \rho_{n_s}\}^T$, $\quad \dot{\mathbf{w}} = \{\dot{w}_1, \dots, \dot{w}_{n_s}\}^T$: mass production rates per volume,

$\rho = \sum_{s=1}^{n_s} \rho_s$, $\quad e_v = \sum_{s=1}^{n_s} \frac{\rho_s}{\rho} e_{v_s}$: mixture vibrational energy per mass,

$p = \sum_{s=1}^{n_s} \frac{\rho_s}{M_s} \bar{R} T$, $\quad \mathbf{e}_v = \{e_{v_1}, \dots, e_{v_{n_s}}\}^T$: vibrational energies per mass,

Q_{t-v} : translational–vibrational energy exchange,

$$E = \frac{|\mathbf{v}|^2}{2} + \sum_{s=1}^{n_s} \frac{\rho_s}{\rho}\left(c_{\mathcal{V}_s} T + e_{v_s} + h_s^o\right)$$

Governing Equations: n_s Species in Vibrational Nonequilibrium

Conservation of mass, momentum, and energy:

Thermochemical source term

$$\frac{\partial \mathbf{U}}{\partial t} + \nabla \cdot \mathbf{F}_c(\mathbf{U}) = -\nabla \cdot \mathbf{F}_p(\mathbf{U}) + \nabla \cdot \mathbf{F}_d(\mathbf{U}) + \mathbf{S}(\mathbf{U}),$$

where

$$\mathbf{U} = \begin{Bmatrix} \boldsymbol{\rho} \\ \rho\mathbf{v} \\ \rho E \\ \rho e_v \end{Bmatrix}, \quad \mathbf{F}_c(\mathbf{U}) = \begin{bmatrix} \boldsymbol{\rho}\mathbf{v}^T \\ \rho\mathbf{v}\mathbf{v}^T \\ \rho E\mathbf{v}^T \\ \rho e_v\mathbf{v}^T \end{bmatrix}, \quad \mathbf{F}_p(\mathbf{U}) = \begin{bmatrix} \mathbf{0} \\ p\mathbf{I} \\ p\mathbf{v}^T \\ \mathbf{0}^T \end{bmatrix}, \quad \mathbf{F}_d(\mathbf{U}) = \begin{bmatrix} -\mathbf{J} \\ \boldsymbol{\tau} \\ \left(\boldsymbol{\tau}\mathbf{v} - \mathbf{q} - \mathbf{q}_v - \mathbf{J}^T\mathbf{h}\right)^T \\ \left(-\mathbf{q}_v - \mathbf{J}^T\mathbf{e}_v\right)^T \end{bmatrix},$$

$$\mathbf{S}(\mathbf{U}) = \begin{Bmatrix} \dot{\mathbf{w}} \\ \mathbf{0} \\ 0 \\ Q_{t-v} + \mathbf{e}_v^T\dot{\mathbf{w}} \end{Bmatrix},$$

$\boldsymbol{\rho} = \{\rho_1, \dots, \rho_{n_s}\}^T$, $\quad \dot{\mathbf{w}} = \{\dot{w}_1, \dots, \dot{w}_{n_s}\}^T$: mass production rates per volume,

$\rho = \sum_{s=1}^{n_s} \rho_s$, $\quad e_v = \sum_{s=1}^{n_s} \frac{\rho_s}{\rho} e_{v_s}$: mixture vibrational energy per mass,

$p = \sum_{s=1}^{n_s} \frac{\rho_s}{M_s} \bar{R}T$, $\quad \mathbf{e}_v = \{e_{v_1}, \dots, e_{v_{n_s}}\}^T$: vibrational energies per mass,

Q_{t-v} : translational–vibrational energy exchange,

$$E = \frac{|\mathbf{v}|^2}{2} + \sum_{s=1}^{n_s} \frac{\rho_s}{\rho}\left(c_{\mathcal{V}_s} T + e_{v_s} + h_s^o\right)$$

Vibrational Energy

Mixture vibrational energy per mass:

$$e_v = \sum_{s=1}^{n_s} \frac{\rho_s}{\rho} e_{v_s},$$

where

$$e_{v_s} = \begin{cases} \sum_{m=1}^{n_{v_s}} e_{v_{s,m}}(T_v) & \text{for molecules,} \\ 0 & \text{for atoms,} \end{cases}$$

and

$$e_{v_{s,m}}(T') = \frac{\bar{R}}{M_s} \frac{\theta_{v_{s,m}}}{\exp\left(\theta_{v_{s,m}}/T'\right) - 1}$$

n_{v_s}: number of vibrational modes of species s ($n_{v_s} = 0$ for atoms)

$\theta_{v_{s,m}}$: characteristic vibrational temperature of mode m of species s

Translational–Vibrational Energy Exchange

Landau–Teller model:

$$Q_{t-v} = \sum_{s=1}^{n_s} \rho_s \sum_{m=1}^{n_{v_s}} \frac{e_{v_{s,m}}(T) - e_{v_{s,m}}(T_v)}{\langle \tau_{s,m} \rangle}$$

Translational–vibrational energy relaxation time for mode m of species s:

$$\langle \tau_{s,m} \rangle = \left(\sum_{s'=1}^{n_s} \frac{y_{s'}}{\tau_{s,m,s'}} \right)^{-1} + \left[\left(N_\text{A} \sum_{s'=1}^{n_s} \frac{\rho_{s'}}{M_{s'}} \right) \sigma_{v_s} \sqrt{\frac{8}{\pi} \frac{\bar{R}T}{M_s}} \right]^{-1},$$

where

$$y_s = \frac{\rho_s / M_s}{\sum_{s'=1}^{n_s} \rho_{s'} / M_{s'}}, \quad \tau_{s,m,s'} = \frac{\exp\left[a_{s,m,s'} \left(T^{-1/3} - b_{s,m,s'} \right) - 18.42 \right]}{p'}, \quad \sigma_{v_s} = \sigma'_{v_s} \left(\frac{50{,}000 \text{ K}}{T} \right)^2$$

p': pressure in atmospheres.

$a_{s,m,s'}$ and $b_{s,m,s'}$: vibrational constants for mode m of species s with colliding species s'

N_A: Avogadro constant

σ_{v_s}: collision-limiting vibrational cross section

σ'_{v_s}: collision-limiting vibrational cross section at 50,000 K.

Chemical Kinetics

Mass production rate per volume for species s: $\dot{w}_s = M_s \sum_{r=1}^{n_r} (\beta_{s,r} - \alpha_{s,r}) (R_{f_r} - R_{b_r})$

Forward and backward reaction rates for reaction r:

$$R_{f_r} = \gamma k_{f_r} \prod_{s=1}^{n_s} \left(\frac{1}{\gamma}\frac{\rho_s}{M_s}\right)^{\alpha_{s,r}} \quad \text{and} \quad R_{b_r} = \gamma k_{b_r} \prod_{s=1}^{n_s} \left(\frac{1}{\gamma}\frac{\rho_s}{M_s}\right)^{\beta_{s,r}}$$

Forward and backward reaction rate coefficients:

$$k_{f_r}(T_c) = C_{f_r} T_c^{\eta_r} \exp\left(-\theta_r/T_c\right) \quad \text{and} \quad k_{b_r}(T) = \frac{k_{f_r}(T)}{K_{e_r}(T)}$$

Equilibrium constant for reaction r:

$$K_{e_r}(T) = \exp\left[A_{1_r}\left(\frac{T}{10,000\text{ K}}\right) + A_{2_r} + A_{3_r}\ln\left(\frac{10,000\text{ K}}{T}\right) + A_{4_r}\frac{10,000\text{ K}}{T} + A_{5_r}\left(\frac{10,000\text{ K}}{T}\right)^2\right]$$

$\alpha_{s,r}$ and $\beta_{s,r}$: stoichiometric coefficients for species s in reaction r

γ: unit conversion factor

C_{f_r}, η_r, A_{i_r}: empirical parameters

θ_r: activation energy of reaction r, divided by Boltzmann constant

T_c: rate-controlling temperature ($T_c = \sqrt{TT_v}$ for dissociation, $T_c = T$ for exchange)

Scope of Code Verification

Conservation of mass, momentum, and energy:

$$\frac{\partial \mathbf{U}}{\partial t} + \nabla \cdot \mathbf{F}_c\left(\mathbf{U}\right) = -\nabla \cdot \mathbf{F}_p\left(\mathbf{U}\right) + \nabla \cdot \mathbf{F}_d\left(\mathbf{U}\right) + \mathbf{S}\left(\mathbf{U}\right),$$

where

$$\mathbf{U} = \begin{Bmatrix} \boldsymbol{\rho} \\ \rho\mathbf{v} \\ \rho E \\ \rho e_v \end{Bmatrix}, \quad \mathbf{F}_c\left(\mathbf{U}\right) = \begin{bmatrix} \boldsymbol{\rho}\mathbf{v}^T \\ \rho\mathbf{v}\mathbf{v}^T \\ \rho E\mathbf{v}^T \\ \rho e_v\mathbf{v}^T \end{bmatrix}, \quad \mathbf{F}_p\left(\mathbf{U}\right) = \begin{bmatrix} \mathbf{0} \\ p\mathbf{I} \\ p\mathbf{v}^T \\ \mathbf{0}^T \end{bmatrix}, \quad \mathbf{F}_d\left(\mathbf{U}\right) = \begin{bmatrix} -\mathbf{J} \\ \boldsymbol{\tau} \\ \left(\boldsymbol{\tau}\mathbf{v} - \mathbf{q} - \mathbf{q}_v - \mathbf{J}^T\mathbf{h}\right)^T \\ \left(-\mathbf{q}_v - \mathbf{J}^T\mathbf{e}_v\right)^T \end{bmatrix},$$

$$\mathbf{S}\left(\mathbf{U}\right) = \begin{Bmatrix} \dot{\mathbf{w}} \\ \mathbf{0} \\ 0 \\ Q_{t-v} + \mathbf{e}_v^T\dot{\mathbf{w}} \end{Bmatrix},$$

$\boldsymbol{\rho} = \left\{\rho_1, \dots, \rho_{n_s}\right\}^T$, $\quad \dot{\mathbf{w}} = \left\{\dot{w}_1, \dots, \dot{w}_{n_s}\right\}^T$: mass production rates per volume,

$\rho = \sum_{s=1}^{n_s} \rho_s$, $\quad e_v = \sum_{s=1}^{n_s} \frac{\rho_s}{\rho} e_{v_s}$: mixture vibrational energy per mass,

$p = \sum_{s=1}^{n_s} \frac{\rho_s}{M_s} \bar{R}T$, $\quad \mathbf{e}_v = \left\{e_{v_1}, \dots, e_{v_{n_s}}\right\}^T$: vibrational energies per mass,

Q_{t-v}: translational–vibrational energy exchange,

$$E = \frac{|\mathbf{v}|^2}{2} + \sum_{s=1}^{n_s} \frac{\rho_s}{\rho}\left(c_{\mathcal{V}_s}T + e_{v_s} + h_s^o\right)$$

Scope of Code Verification

Conservation of mass, momentum, and energy:

$$\frac{\partial \mathbf{U}}{\partial t} + \underbrace{\nabla \cdot \mathbf{F}_c(\mathbf{U}) = -\nabla \cdot \mathbf{F}_p(\mathbf{U})}_{\text{Non-diffusive flux gradients}} + \nabla \cdot \mathbf{F}_d(\mathbf{U}) + \underbrace{\mathbf{S}(\mathbf{U})}_{\text{Thermochemical source term}},$$

where

$$\mathbf{U} = \begin{Bmatrix} \boldsymbol{\rho} \\ \rho\mathbf{v} \\ \rho E \\ \rho e_v \end{Bmatrix}, \quad \mathbf{F}_c(\mathbf{U}) = \begin{bmatrix} \boldsymbol{\rho}\mathbf{v}^T \\ \rho\mathbf{v}\mathbf{v}^T \\ \rho E\mathbf{v}^T \\ \rho e_v\mathbf{v}^T \end{bmatrix}, \quad \mathbf{F}_p(\mathbf{U}) = \begin{bmatrix} \mathbf{0} \\ p\mathbf{I} \\ p\mathbf{v}^T \\ \mathbf{0}^T \end{bmatrix}, \quad \mathbf{F}_d(\mathbf{U}) = \begin{bmatrix} -\mathbf{J} \\ \boldsymbol{\tau} \\ \left(\boldsymbol{\tau}\mathbf{v} - \mathbf{q} - \mathbf{q}_v - \mathbf{J}^T\mathbf{h}\right)^T \\ \left(-\mathbf{q}_v - \mathbf{J}^T\mathbf{e}_v\right)^T \end{bmatrix},$$

$$\mathbf{S}(\mathbf{U}) = \begin{Bmatrix} \dot{\mathbf{w}} \\ \mathbf{0} \\ 0 \\ Q_{t-v} + \mathbf{e}_v^T\dot{\mathbf{w}} \end{Bmatrix},$$

$\boldsymbol{\rho} = \{\rho_1, \dots, \rho_{n_s}\}^T$, $\dot{\mathbf{w}} = \{\dot{w}_1, \dots, \dot{w}_{n_s}\}^T$: mass production rates per volume,

$\rho = \sum_{s=1}^{n_s} \rho_s$, $e_v = \sum_{s=1}^{n_s} \frac{\rho_s}{\rho} e_{v_s}$: mixture vibrational energy per mass,

$p = \sum_{s=1}^{n_s} \frac{\rho_s}{M_s} \bar{R} T$, $\mathbf{e}_v = \{e_{v_1}, \dots, e_{v_{n_s}}\}^T$: vibrational energies per mass,

Q_{t-v} : translational–vibrational energy exchange,

$$E = \frac{|\mathbf{v}|^2}{2} + \sum_{s=1}^{n_s} \frac{\rho_s}{\rho}\left(c_{\mathcal{V}_s} T + e_{v_s} + h_s^o\right)$$

Scope of Code Verification

Conservation of mass, momentum, and energy:

Non-diffusive flux gradients

$$\frac{\partial \mathbf{U}}{\partial t} + \nabla \cdot \mathbf{F}_c(\mathbf{U}) = -\nabla \cdot \mathbf{F}_p(\mathbf{U}) + \nabla \cdot \mathbf{F}_d(\mathbf{U}) + \mathbf{S}(\mathbf{U}),$$

Spatial discretization

where

$$\mathbf{U} = \begin{Bmatrix} \boldsymbol{\rho} \\ \rho\mathbf{v} \\ \rho E \\ \rho e_v \end{Bmatrix}, \quad \mathbf{F}_c(\mathbf{U}) = \begin{bmatrix} \boldsymbol{\rho}\mathbf{v}^T \\ \rho\mathbf{v}\mathbf{v}^T \\ \rho E\mathbf{v}^T \\ \rho e_v\mathbf{v}^T \end{bmatrix}, \quad \mathbf{F}_p(\mathbf{U}) = \begin{bmatrix} \mathbf{0} \\ p\mathbf{I} \\ p\mathbf{v}^T \\ \mathbf{0}^T \end{bmatrix}, \quad \mathbf{F}_d(\mathbf{U}) = \begin{bmatrix} -\mathbf{J} \\ \boldsymbol{\tau} \\ \left(\boldsymbol{\tau}\mathbf{v} - \mathbf{q} - \mathbf{q}_v - \mathbf{J}^T\mathbf{h}\right)^T \\ \left(-\mathbf{q}_v - \mathbf{J}^T\mathbf{e}_v\right)^T \end{bmatrix},$$

$$\mathbf{S}(\mathbf{U}) = \begin{Bmatrix} \dot{\mathbf{w}} \\ \mathbf{0} \\ 0 \\ Q_{t-v} + \mathbf{e}_v^T\dot{\mathbf{w}} \end{Bmatrix},$$

$\boldsymbol{\rho} = \{\rho_1, \dots, \rho_{n_s}\}^T$, $\quad \dot{\mathbf{w}} = \{\dot{w}_1, \dots, \dot{w}_{n_s}\}^T$: mass production rates per volume,

$\rho = \sum_{s=1}^{n_s} \rho_s$, $\quad e_v = \sum_{s=1}^{n_s} \frac{\rho_s}{\rho} e_{v_s}$: mixture vibrational energy per mass,

$p = \sum_{s=1}^{n_s} \frac{\rho_s}{M_s} \bar{R} T$, $\quad \mathbf{e}_v = \{e_{v_1}, \dots, e_{v_{n_s}}\}^T$: vibrational energies per mass,

Q_{t-v} : translational–vibrational energy exchange,

$$E = \frac{|\mathbf{v}|^2}{2} + \sum_{s=1}^{n_s} \frac{\rho_s}{\rho}\left(c_{\mathcal{V}_s} T + e_{v_s} + h_s^o\right)$$

Scope of Code Verification

Conservation of mass, momentum, and energy:

Thermochemical source term

$$\frac{\partial \mathbf{U}}{\partial t} + \nabla \cdot \mathbf{F}_c(\mathbf{U}) = -\nabla \cdot \mathbf{F}_p(\mathbf{U}) + \nabla \cdot \mathbf{F}_d(\mathbf{U}) + \mathbf{S}(\mathbf{U}),$$

where

Implementation

$$\mathbf{U} = \begin{Bmatrix} \boldsymbol{\rho} \\ \rho\mathbf{v} \\ \rho E \\ \rho e_v \end{Bmatrix}, \quad \mathbf{F}_c(\mathbf{U}) = \begin{bmatrix} \boldsymbol{\rho}\mathbf{v}^T \\ \rho\mathbf{v}\mathbf{v}^T \\ \rho E\mathbf{v}^T \\ \rho e_v\mathbf{v}^T \end{bmatrix}, \quad \mathbf{F}_p(\mathbf{U}) = \begin{bmatrix} \mathbf{0} \\ p\mathbf{I} \\ p\mathbf{v}^T \\ \mathbf{0}^T \end{bmatrix}, \quad \mathbf{F}_d(\mathbf{U}) = \begin{bmatrix} -\mathbf{J} \\ \boldsymbol{\tau} \\ (\boldsymbol{\tau}\mathbf{v} - \mathbf{q} - \mathbf{q}_v - \mathbf{J}^T\mathbf{h})^T \\ (-\mathbf{q}_v - \mathbf{J}^T\mathbf{e}_v)^T \end{bmatrix},$$

$$\mathbf{S}(\mathbf{U}) = \begin{Bmatrix} \dot{\mathbf{w}} \\ \mathbf{0} \\ 0 \\ Q_{t-v} + \mathbf{e}_v^T\dot{\mathbf{w}} \end{Bmatrix},$$

$\boldsymbol{\rho} = \{\rho_1, \dots, \rho_{n_s}\}^T$,

$\rho = \sum_{s=1}^{n_s} \rho_s$,

$p = \sum_{s=1}^{n_s} \frac{\rho_s}{M_s}\bar{R}T$,

$\dot{\mathbf{w}} = \{\dot{w}_1, \dots, \dot{w}_{n_s}\}^T$: mass production rates per volume,

$e_v = \sum_{s=1}^{n_s} \frac{\rho_s}{\rho} e_{v_s}$: mixture vibrational energy per mass,

$\mathbf{e}_v = \{e_{v_1}, \dots, e_{v_{n_s}}\}^T$: vibrational energies per mass,

Q_{t-v} : translational–vibrational energy exchange,

$$E = \frac{|\mathbf{v}|^2}{2} + \sum_{s=1}^{n_s} \frac{\rho_s}{\rho}\left(c_{\mathcal{V}_s} T + e_{v_s} + h_s^o\right)$$

Outline

- Introduction
- Governing Equations
- Verification Techniques for Spatial Accuracy
  - Spatial Accuracy
  - Solutions
  - Error Norms
- Spatial-Discretization Verification Results
- Verification Techniques for Thermochemical Source Term
- Thermochemical-Source-Term Verification Results
- Summary

Spatial Accuracy (Steady State)

Governing equations
$\mathbf{r}(\mathbf{U}) = \mathbf{0}$

Discretized equations
$\mathbf{r}_h(\mathbf{U}_h) = \mathbf{0}$

Discretization error is $\mathbf{e}_h = \mathbf{U}_h - \mathbf{U}$

Truncation error is $\boldsymbol{\tau}_h(\mathbf{V}) = \mathbf{r}_h(\mathbf{V}) - \mathbf{r}(\mathbf{V})$

Letting $\mathbf{V} = \mathbf{U}_h$ and adding $\mathbf{r}(\mathbf{U}) = \mathbf{0}$,

$$\boldsymbol{\tau}_h(\mathbf{U}_h) = \mathbf{r}_h(\mathbf{U}_h) - \mathbf{r}(\mathbf{U}_h) + \mathbf{r}(\mathbf{U}) = \mathbf{r}(\mathbf{U}) - \mathbf{r}(\mathbf{U}_h)$$

When $\mathbf{r}$ is linearized w.r.t. $\mathbf{U}$, $\mathbf{r}(\mathbf{e}_h) = -\boldsymbol{\tau}_h(\mathbf{U}_h)$

Spatial Accuracy (Steady State)

For p^{th}-order-accurate discretization, truncation error is

$$\boldsymbol{\tau}_h = \mathbf{r}(\mathbf{U}) - \mathbf{r}(\mathbf{U}_h) = \mathbf{C}_\mathbf{r} h^p + \mathcal{O}(h^{p+1})$$

h: relative characterization of cell sizes

- Between meshes, with respect to one dimension
- Individual cell sizes may be non-uniform functions of h
- Sufficiently fine meshes $\rightarrow$ asymptotic region ($h^{p+1} \ll h^p$)

$$\mathbf{e}_h = \mathbf{U}_h - \mathbf{U} \approx \mathbf{C}_\mathbf{U} h^p$$

$\mathbf{C}_\mathbf{r}$ and $\mathbf{C}_\mathbf{U}$: function of derivative(s) of state vector $\mathbf{U}$

- Approximately constant between meshes in asymptotic region

Order of Accuracy

Observed accuracy p computed using 2 meshes:

Order of Accuracy

Observed accuracy p computed using 2 meshes:

Coarser mesh (h)

$$e_1 = Ch^p$$

Order of Accuracy

Observed accuracy p computed using 2 meshes:

Coarser mesh (h)

$$e_1 = Ch^p$$

Finer mesh (h/q)
(q-times as fine in each dimension)

$$e_2 = C(h/q)^p$$

Order of Accuracy

Observed accuracy p computed using 2 meshes:

Coarser mesh (h)

$$e_1 = Ch^p$$

Finer mesh (h/q)
(q-times as fine in each dimension)

$$e_2 = C(h/q)^p$$

p is computed by

$$p \approx \frac{\log |e_1/e_2|}{\log q} = \log_q |e_1/e_2|$$

Solutions

Need solution to compute error

Solutions

Exact Solutions

Solutions

Exact Solutions

- Negligible implementation effort: $\mathbf{r}(\mathbf{U}_{\text{Exact}}) = \mathbf{0}$

Solutions

Exact Solutions

- Negligible implementation effort: $\mathbf{r}(\mathbf{U}_{\text{Exact}}) = \mathbf{0}$
- Limited cases

Solutions

Exact Solutions

- Negligible implementation effort: $\mathbf{r}(\mathbf{U}_{\text{Exact}}) = \mathbf{0}$
- Limited cases
- Span small subset of application space

Solutions

Exact Solutions

- Negligible implementation effort: $\mathbf{r}(\mathbf{U}_{\text{Exact}}) = \mathbf{0}$
- Limited cases
- Span small subset of application space

Manufactured Solutions

Solutions

Exact Solutions

- Negligible implementation effort: $\mathbf{r}(\mathbf{U}_{\text{Exact}}) = \mathbf{0}$
- Limited cases
- Span small subset of application space

Manufactured Solutions

- Do not satisfy original equations: $\mathbf{r}(\mathbf{U}_{\text{MS}}) \neq \mathbf{0}$

Solutions

Exact Solutions

- Negligible implementation effort: $\mathbf{r}(\mathbf{U}_{\text{Exact}}) = \mathbf{0}$
- Limited cases
- Span small subset of application space

Manufactured Solutions

- Do not satisfy original equations: $\mathbf{r}(\mathbf{U}_{\text{MS}}) \neq \mathbf{0}$
- Require source term: $\mathbf{r}_h(\mathbf{U}_h) = \mathbf{r}(\mathbf{U}_{\text{MS}})$

Solutions

Exact Solutions

- Negligible implementation effort: $\mathbf{r}(\mathbf{U}_{\text{Exact}}) = \mathbf{0}$
- Limited cases
- Span small subset of application space

Manufactured Solutions

- Do not satisfy original equations: $\mathbf{r}(\mathbf{U}_{\text{MS}}) \neq \mathbf{0}$
- Require source term: $\mathbf{r}_h(\mathbf{U}_h) = \mathbf{r}(\mathbf{U}_{\text{MS}})$
- Manufactured to exercise features of interest

Solutions

Exact Solutions

- Negligible implementation effort: $\mathbf{r}(\mathbf{U}_{\text{Exact}}) = \mathbf{0}$
- Limited cases
- Span small subset of application space

Manufactured Solutions

- Do not satisfy original equations: $\mathbf{r}(\mathbf{U}_{\text{MS}}) \neq \mathbf{0}$
- Require source term: $\mathbf{r}_h(\mathbf{U}_h) = \mathbf{r}(\mathbf{U}_{\text{MS}})$
- Manufactured to exercise features of interest
- Should be smooth, continuously differentiable functions with generally nonzero derivatives and moderate variations

Solutions

Exact Solutions

- Negligible implementation effort: $\mathbf{r}(\mathbf{U}_{\text{Exact}}) = \mathbf{0}$
- Limited cases
- Span small subset of application space

Manufactured Solutions

- Do not satisfy original equations: $\mathbf{r}(\mathbf{U}_{\text{MS}}) \neq \mathbf{0}$
- Require source term: $\mathbf{r}_h(\mathbf{U}_h) = \mathbf{r}(\mathbf{U}_{\text{MS}})$
- Manufactured to exercise features of interest
- Should be smooth, continuously differentiable functions with generally nonzero derivatives and moderate variations

Solutions

Exact Solutions

- Negligible implementation effort: $\mathbf{r}(\mathbf{U}_{\text{Exact}}) = \mathbf{0}$
- Limited cases
- Span small subset of application space

Manufactured Solutions

- Do not satisfy original equations: $\mathbf{r}(\mathbf{U}_{\text{MS}}) \neq \mathbf{0}$
- Require source term: $\mathbf{r}_h(\mathbf{U}_h) = \mathbf{r}(\mathbf{U}_{\text{MS}})$
- Manufactured to exercise features of interest
- Should be smooth, continuously differentiable functions with generally nonzero derivatives and moderate variations

Error Norms

Computing p at a single location in domain has two shortcomings:

Error Norms

Computing p at a single location in domain has two shortcomings:

- For cell-centered schemes, cell centers vary with mesh refinement

Error Norms

Computing p at a single location in domain has two shortcomings:

- For cell-centered schemes, cell centers vary with mesh refinement
- In regions where error vanishes, computed p is meaningless

Error Norms

Computing p at a single location in domain has two shortcomings:

- For cell-centered schemes, cell centers vary with mesh refinement
- In regions where error vanishes, computed p is meaningless

Error norms to quantify spatial accuracy: $p = \log_q \left(\varepsilon_{\alpha_1} / \varepsilon_{\alpha_2} \right)$

Error Norms

Computing p at a single location in domain has two shortcomings:

- For cell-centered schemes, cell centers vary with mesh refinement
- In regions where error vanishes, computed p is meaningless

Error norms to quantify spatial accuracy: $p = \log_q\left(\varepsilon_{\alpha_1}/\varepsilon_{\alpha_2}\right)$

- L^1-norm: $\varepsilon_\alpha^1 = \|\alpha_h(\mathbf{x}) - \alpha(\mathbf{x})\|_1 = \int_\Omega |\alpha_h(\mathbf{x}) - \alpha(\mathbf{x})| d\Omega$

Error Norms

Computing p at a single location in domain has two shortcomings:

- For cell-centered schemes, cell centers vary with mesh refinement
- In regions where error vanishes, computed p is meaningless

Error norms to quantify spatial accuracy: $p = \log_q\left(\varepsilon_{\alpha_1}/\varepsilon_{\alpha_2}\right)$

- L^1-norm: $\varepsilon_\alpha^1 = \|\alpha_h(\mathbf{x}) - \alpha(\mathbf{x})\|_1 = \int_\Omega |\alpha_h(\mathbf{x}) - \alpha(\mathbf{x})| d\Omega$
  - Average error

Error Norms

Computing p at a single location in domain has two shortcomings:

- For cell-centered schemes, cell centers vary with mesh refinement
- In regions where error vanishes, computed p is meaningless

Error norms to quantify spatial accuracy: $p = \log_q \left(\varepsilon_{\alpha_1} / \varepsilon_{\alpha_2} \right)$

- L^1-norm: $\varepsilon_\alpha^1 = \|\alpha_h(\mathbf{x}) - \alpha(\mathbf{x})\|_1 = \int_\Omega |\alpha_h(\mathbf{x}) - \alpha(\mathbf{x})| d\Omega$
  - Average error
  - Not significantly contaminated by localized deviations (e.g., discontinuities, lower-order boundary conditions)

Error Norms

Computing p at a single location in domain has two shortcomings:

- For cell-centered schemes, cell centers vary with mesh refinement
- In regions where error vanishes, computed p is meaningless

Error norms to quantify spatial accuracy: $p = \log_q \left(\varepsilon_{\alpha_1}/\varepsilon_{\alpha_2}\right)$

- L^1-norm: $\varepsilon_\alpha^1 = \|\alpha_h(\mathbf{x}) - \alpha(\mathbf{x})\|_1 = \int_\Omega |\alpha_h(\mathbf{x}) - \alpha(\mathbf{x})| d\Omega$
  - Average error
  - Not significantly contaminated by localized deviations (e.g., discontinuities, lower-order boundary conditions)
- L^∞-norm: $\varepsilon_\alpha^\infty = \|\alpha_h(\mathbf{x}) - \alpha(\mathbf{x})\|_\infty = \max_{\mathbf{x}\in\Omega} |\alpha_h(\mathbf{x}) - \alpha(\mathbf{x})|$

Error Norms

Computing p at a single location in domain has two shortcomings:

- For cell-centered schemes, cell centers vary with mesh refinement
- In regions where error vanishes, computed p is meaningless

Error norms to quantify spatial accuracy: $p = \log_q \left(\varepsilon_{\alpha_1}/\varepsilon_{\alpha_2}\right)$

- L^1-norm: $\varepsilon_\alpha^1 = \|\alpha_h(\mathbf{x}) - \alpha(\mathbf{x})\|_1 = \int_\Omega |\alpha_h(\mathbf{x}) - \alpha(\mathbf{x})| d\Omega$
  - Average error
  - Not significantly contaminated by localized deviations (e.g., discontinuities, lower-order boundary conditions)
- L^∞-norm: $\varepsilon_\alpha^\infty = \|\alpha_h(\mathbf{x}) - \alpha(\mathbf{x})\|_\infty = \max_{\mathbf{x}\in\Omega} |\alpha_h(\mathbf{x}) - \alpha(\mathbf{x})|$
  - Maximum error

Error Norms

Computing p at a single location in domain has two shortcomings:

- For cell-centered schemes, cell centers vary with mesh refinement
- In regions where error vanishes, computed p is meaningless

Error norms to quantify spatial accuracy: $p = \log_q \left(\varepsilon_{\alpha_1} / \varepsilon_{\alpha_2} \right)$

- L^1-norm: $\varepsilon_\alpha^1 = \|\alpha_h(\mathbf{x}) - \alpha(\mathbf{x})\|_1 = \int_\Omega |\alpha_h(\mathbf{x}) - \alpha(\mathbf{x})| d\Omega$
  - Average error
  - Not significantly contaminated by localized deviations (e.g., discontinuities, lower-order boundary conditions)
- L^∞-norm: $\varepsilon_\alpha^\infty = \|\alpha_h(\mathbf{x}) - \alpha(\mathbf{x})\|_\infty = \max_{\mathbf{x}\in\Omega} |\alpha_h(\mathbf{x}) - \alpha(\mathbf{x})|$
  - Maximum error
  - Catches localized deviations (expected and **unexpected**)

Error Norms

Computing p at a single location in domain has two shortcomings:

- For cell-centered schemes, cell centers vary with mesh refinement
- In regions where error vanishes, computed p is meaningless

Error norms to quantify spatial accuracy: $p = \log_q\left(\varepsilon_{\alpha_1}/\varepsilon_{\alpha_2}\right)$

- L^1-norm: $\varepsilon^1_\alpha = \|\alpha_h(\mathbf{x}) - \alpha(\mathbf{x})\|_1 = \int_\Omega |\alpha_h(\mathbf{x}) - \alpha(\mathbf{x})| d\Omega$
  - Average error
  - Not significantly contaminated by localized deviations (e.g., discontinuities, lower-order boundary conditions)
- L^∞-norm: $\varepsilon^\infty_\alpha = \|\alpha_h(\mathbf{x}) - \alpha(\mathbf{x})\|_\infty = \max_{\mathbf{x}\in\Omega} |\alpha_h(\mathbf{x}) - \alpha(\mathbf{x})|$
  - Maximum error
  - Catches localized deviations (expected and **unexpected**)
- Without discontinuities, both norms should yield same p

Outline

- Introduction
- Governing Equations
- Verification Techniques for Spatial Accuracy
- Spatial-Discretization Verification Results
  - Single-Species Inviscid Flow in Thermochemical Equilibrium
  - Five-Species Inviscid Flow in Chemical Nonequilibrium
- Verification Techniques for Thermochemical Source Term
- Thermochemical-Source-Term Verification Results
- Summary

1D Supersonic Flow using a Manufactured Solution

- One-dimensional domain: $x \in [0, 1]$ m
- Boundary conditions:
  - Supersonic inflow ($x = 0$ m)
  - Supersonic outflow ($x = 1$ m)
- 5 uniform meshes: 50, 100, 200, 400, 800 elements
- Solution consists of small, smooth perturbations to uniform flow:

$$
\begin{aligned}
\rho(x) &= \bar{\rho}\left[1 - \epsilon \sin(\pi x)\right], \\
u(x) &= \bar{u}\left[1 - \epsilon \sin(\pi x)\right], \\
T(x) &= \bar{T}\left[1 + \epsilon \sin(\pi x)\right],
\end{aligned}
$$

$\bar{\rho} = 1$ kg/m^3, $\bar{T} = 300$ K, $\bar{M} = 2.5$, $\epsilon = 0.05$

1D Supersonic Flow using a Manufactured Solution

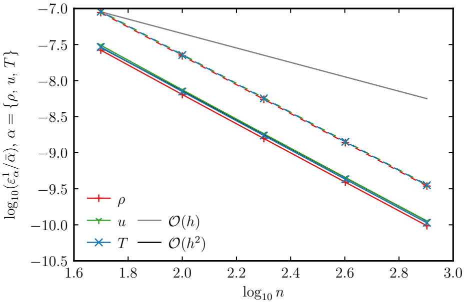

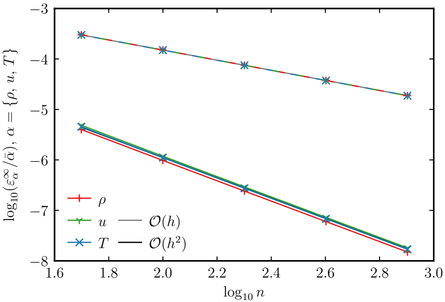

	First-order accurate			Second-order accurate		
	Original boundary conditions			Corrected boundary conditions		
Mesh	ρ	u	T	ρ	u	T
1–2	1.0008	1.0008	1.0008	2.0313	2.0362	2.0351
2–3	1.0002	1.0002	1.0002	2.0157	2.0184	2.0178
3–4	1.0001	1.0001	1.0000	2.0079	2.0093	2.0090
4–5	1.0000	1.0000	1.0000	2.0040	2.0047	2.0045

Observed accuracy p using L^∞-norms of the error

2D Supersonic Flow using a Manufactured Solution

- Two-dimensional domain: $(x, y) \in [0,\, 1]\ \mathrm{m} \times [0,\, 1]\ \mathrm{m}$
- Boundary conditions:
  - Supersonic inflow ($x = 0$ m)
  - Supersonic outflow ($x = 1$ m)
  - Slip wall (tangent flow) ($y = 0$ m & $y = 1$ m)
- 5 nonuniform meshes: $25 \times 25 \rightarrow 400 \times 400$
- Solution consists of small, smooth perturbations to uniform flow:

$$\rho\,(x, y) = \bar{\rho}\,\left[1 - \epsilon \sin\left(\tfrac{5}{4}\pi x\right)\left(\sin\left(\ \pi y\right) + \cos\left(\ \pi y\right)\right)\right],$$

$$u\,(x, y) = \bar{u}\,\left[1 + \epsilon \sin\left(\tfrac{1}{4}\pi x\right)\left(\sin\left(\ \pi y\right) + \cos\left(\ \pi y\right)\right)\right],$$

$$v\,(x, y) = \bar{v}\,\left[\ \ - \epsilon \sin\left(\tfrac{5}{4}\pi x\right)\left(\sin\left(\ \pi y\right) \qquad\qquad\qquad \right)\right],$$

$$T(x, y) = \bar{T}\left[1 + \epsilon \sin\left(\tfrac{5}{4}\pi x\right)\left(\sin\left(\ \pi y\right) + \cos\left(\ \pi y\right)\right)\right],$$

$\bar{\rho} = 1\ \mathrm{kg/m^3}$, $\bar{T} = 300$ K, $\bar{M} = 2.5$, $\epsilon = 0.05$

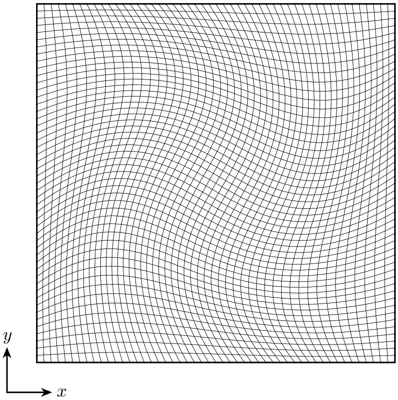

2D Supersonic Flow using a Manufactured Solution

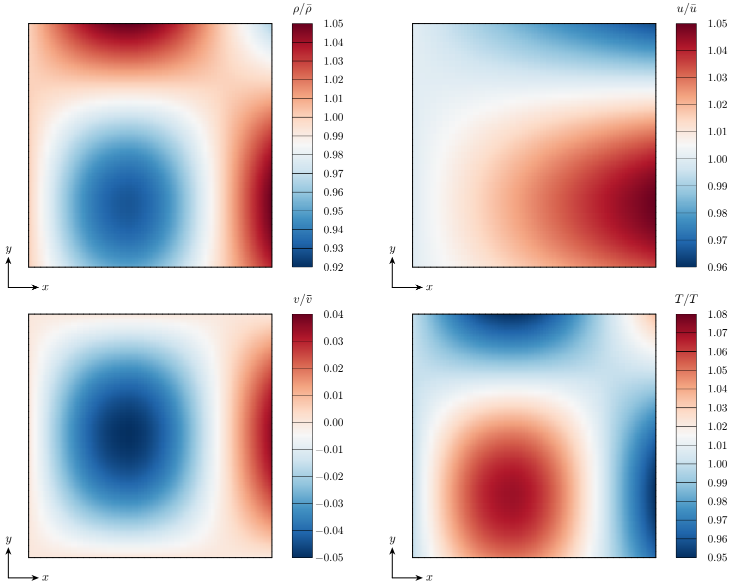

2D Supersonic Flow using a Manufactured Solution

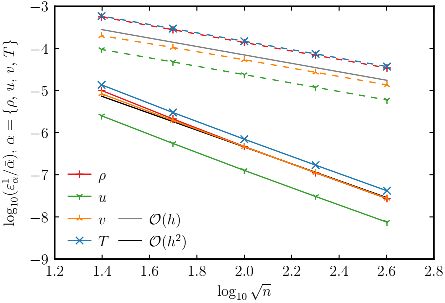

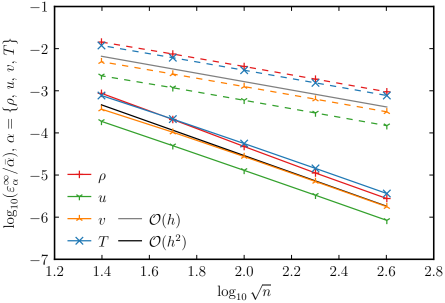

	First-order accurate				Second-order accurate			
	Original boundary conditions				Corrected boundary conditions			
Mesh	ρ	u	v	T	ρ	u	v	T
1–2	0.9420	0.9409	0.9721	0.9628	2.0623	1.9188	1.8174	1.8598
2–3	0.9850	0.9902	0.9910	0.9874	2.1304	1.9450	1.9221	1.9280
3–4	0.9960	1.0002	0.9924	0.9952	2.0902	1.9603	1.9671	1.9586
4–5	0.9989	1.0009	0.9959	0.9984	2.0128	1.9823	1.9860	1.9809

Observed accuracy p using L^∞-norms of the error

2D Supersonic Flow using an Exact Solution

- Two-dimensional domain: $(r, \theta) \in [1,\ 1.384] \times [0,\ 90]^\circ$
- Boundary conditions:
  - Supersonic inflow ($\theta = 90^\circ$)
  - Supersonic outflow ($\theta = 0^\circ$)
  - Slip wall (tangent flow) ($r = 1$ & $r = 1.384$)
- 6 meshes: $32 \times 8 \to 1024 \times 256$
- Solution is steady isentropic vortex:

$$\rho(r) = \rho_i \left[1 + \frac{\gamma - 1}{2} M_i^2 \left(1 - \left(\frac{r_i}{r}\right)^2\right)\right]^{\frac{1}{\gamma-1}},$$

$$u_r(r) = 0,$$

$$u_\theta(r) = -a_i M_i \frac{r_i}{r},$$

$$T(r) = T_i \left[1 + \frac{\gamma - 1}{2} M_i^2 \left(1 - \left(\frac{r_i}{r}\right)^2\right)\right],$$

$\rho_i = 1,\ a_i = 1,\ M_i = 2.25,\ T_i = 1/(\gamma R)$

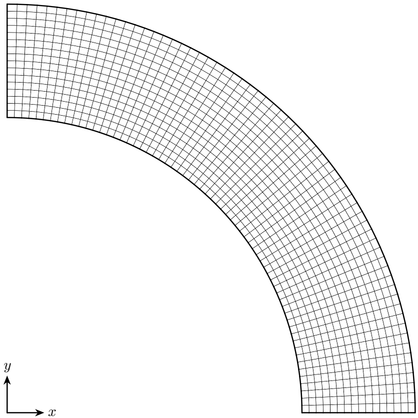

2D Supersonic Flow using an Exact Solution

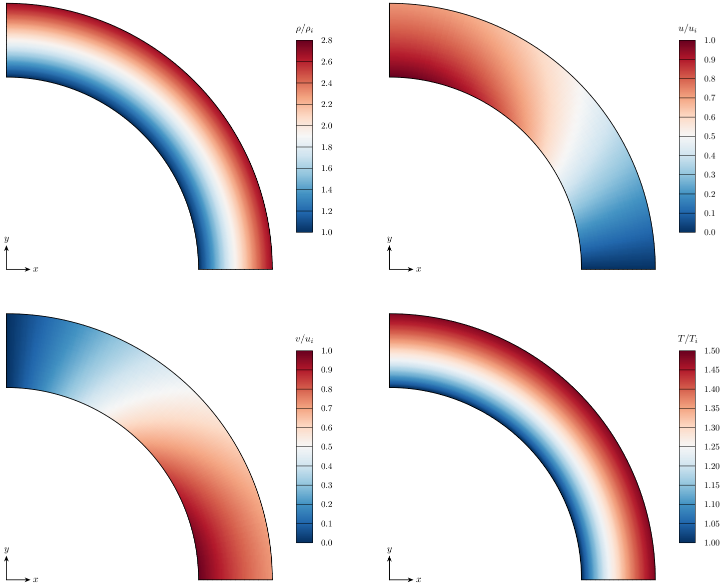

2D Supersonic Flow using an Exact Solution

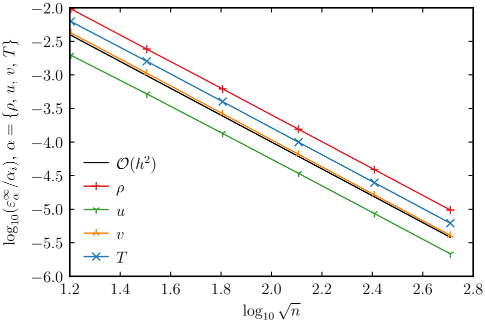

Mesh	ρ	u	v	T
1–2	1.9896	1.9119	1.9943	1.9699
2–3	1.9735	1.9589	2.0070	1.9979
3–4	1.9954	1.9760	2.0099	2.0076
4–5	1.9972	1.9879	2.0054	2.0044
5–6	1.9986	1.9940	2.0029	2.0025

Observed accuracy p using L^∞-norms of the error

3D Supersonic Flow using a Manufactured Solution

- Three-dimensional domain: $(x, y, z) \in [0,\ 1]\ \mathrm{m} \times [0,\ 1]\ \mathrm{m} \times [0,\ 1]\ \mathrm{m}$
- Boundary conditions:
  - Supersonic inflow ($x = 0$ m)
  - Supersonic outflow ($x = 1$ m)
  - Slip wall (tangent flow) ($y = 0$ m, $y = 1$ m, $z = 0$ m, $z = 1$ m)
- 5 nonuniform meshes: $25 \times 25 \times 25 \rightarrow 400 \times 400 \times 400$
- Solution consists of small, smooth perturbations to uniform flow:

$$
\begin{aligned}
\rho(x,y,z) &= \bar{\rho}\left[1 - \epsilon \sin\left(\tfrac{5}{4}\pi x\right)\left(\sin(\pi y) + \cos(\pi y)\right)\left(\sin(\pi z) + \cos(\pi z)\right)\right],\\
u(x,y,z) &= \bar{u}\left[1 + \epsilon \sin\left(\tfrac{1}{4}\pi x\right)\left(\sin(\pi y) + \cos(\pi y)\right)\left(\sin(\pi z) + \cos(\pi z)\right)\right],\\
v(x,y,z) &= \bar{v}\left[\ \ - \epsilon \sin\left(\tfrac{5}{4}\pi x\right)\left(\sin(\pi y)\right)\left(\sin(\pi z) + \cos(\pi z)\right)\right],\\
w(x,y,z) &= \bar{w}\left[\ \ - \epsilon \sin\left(\tfrac{5}{4}\pi x\right)\left(\sin(\pi y) + \cos(\pi y)\right)\left(\sin(\pi z)\right)\right],\\
T(x,y,z) &= \bar{T}\left[1 + \epsilon \sin\left(\tfrac{5}{4}\pi x\right)\left(\sin(\pi y) + \cos(\pi y)\right)\left(\sin(\pi z) + \cos(\pi z)\right)\right],
\end{aligned}
$$

$\bar{\rho} = 1\ \mathrm{kg/m^3}$, $\bar{T} = 300$ K, $\bar{M} = 2.5$, $\epsilon = 0.05$

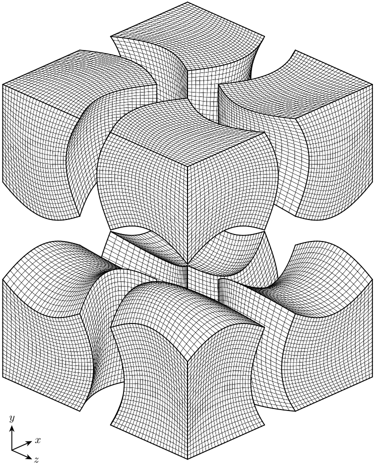

3D Supersonic Flow using a Manufactured Solution

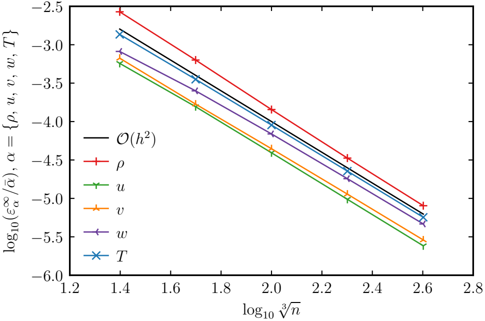

Mesh	ρ	u	v	w	T
1–2	2.0849	1.8731	1.9841	1.7039	1.9404
2–3	2.1406	1.9923	1.9295	1.8621	1.9774
3–4	2.0990	2.0115	1.9623	1.9349	1.9922
4–5	2.0585	2.0100	1.9820	1.9571	1.9964

Observed accuracy p using L^∞-norms of the error

Five-Species Air Model

5 species: N_2, O_2, NO, N, and O

17 reactions:

r	Reaction		Type of Reaction
1–5	$N_2 + \mathcal{M} \leftrightharpoons N + N + \mathcal{M}$,	$\mathcal{M} = \{N_2, O_2, NO, N, O\}$	Dissociation
6–10	$O_2 + \mathcal{M} \leftrightharpoons O + O + \mathcal{M}$,	$\mathcal{M} = \{N_2, O_2, NO, N, O\}$	Dissociation
11–15	$NO + \mathcal{M} \leftrightharpoons N + O + \mathcal{M}$,	$\mathcal{M} = \{N_2, O_2, NO, N, O\}$	Dissociation
16	$N_2 + O \leftrightharpoons N + NO$		Exchange
17	$NO + O \leftrightharpoons N + O_2$		Exchange

Five-Species Inviscid Flow in Chemical Nonequilibrium

- Two-dimensional domain: $(x, y) \in [0,\, 1]$ m $\times$ $[0,\, 1]$ m
- Same boundary conditions
- 7 nonuniform meshes: $25 \times 25 \to 1600 \times 1600$
- Solution consists of small, smooth perturbations to uniform flow

$$
\begin{aligned}
\rho_{\mathrm{N}_2}(x,y) &= \bar{\rho}_{\mathrm{N}_2}\left[1 - \epsilon \sin\left(\tfrac{5}{4}\pi x\right)\left(\sin\left(\pi y\right) + \cos\left(\pi y\right)\right)\right],\\
\rho_{\mathrm{O}_2}(x,y) &= \bar{\rho}_{\mathrm{O}_2}\left[1 + \epsilon \sin\left(\tfrac{3}{4}\pi x\right)\left(\sin\left(\pi y\right) + \cos\left(\pi y\right)\right)\right],\\
\rho_{\mathrm{NO}}(x,y) &= \bar{\rho}_{\mathrm{NO}}\left[1 + \epsilon \sin\left(\pi x\right)\left(\sin\left(\pi y\right)\right)\right],\\
\rho_{\mathrm{N}}(x,y) &= \bar{\rho}_{\mathrm{N}}\left[1 + \epsilon \sin\left(\pi x\right)\left(\cos\left(\tfrac{1}{4}\pi y\right)\right)\right],\\
\rho_{\mathrm{O}}(x,y) &= \bar{\rho}_{\mathrm{O}}\left[1 + \epsilon \sin\left(\pi x\right)\left(\sin\left(\pi y\right) + \cos\left(\tfrac{1}{4}\pi y\right)\right)\right],\\
u(x,y) &= \bar{u}\left[1 + \epsilon \sin\left(\tfrac{1}{4}\pi x\right)\left(\sin\left(\pi y\right) + \cos\left(\pi y\right)\right)\right],\\
v(x,y) &= \bar{v}\left[- \epsilon \sin\left(\tfrac{5}{4}\pi x\right)\left(\sin\left(\pi y\right)\right)\right],\\
T(x,y) &= \bar{T}\left[1 + \epsilon \sin\left(\tfrac{5}{4}\pi x\right)\left(\sin\left(\pi y\right) + \cos\left(\pi y\right)\right)\right],\\
T_v(x,y) &= \bar{T}_v\left[1 + \epsilon \sin\left(\tfrac{3}{4}\pi x\right)\left(\sin\left(\tfrac{5}{4}\pi y\right) + \cos\left(\tfrac{3}{4}\pi y\right)\right)\right]
\end{aligned}
$$

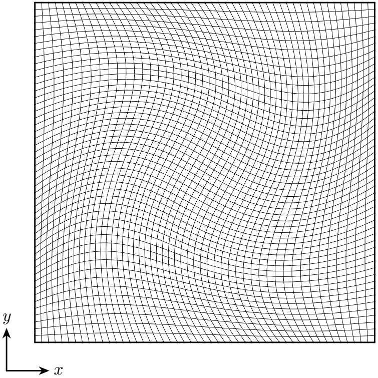

Five-Species Inviscid Flow in Chemical Nonequilibrium

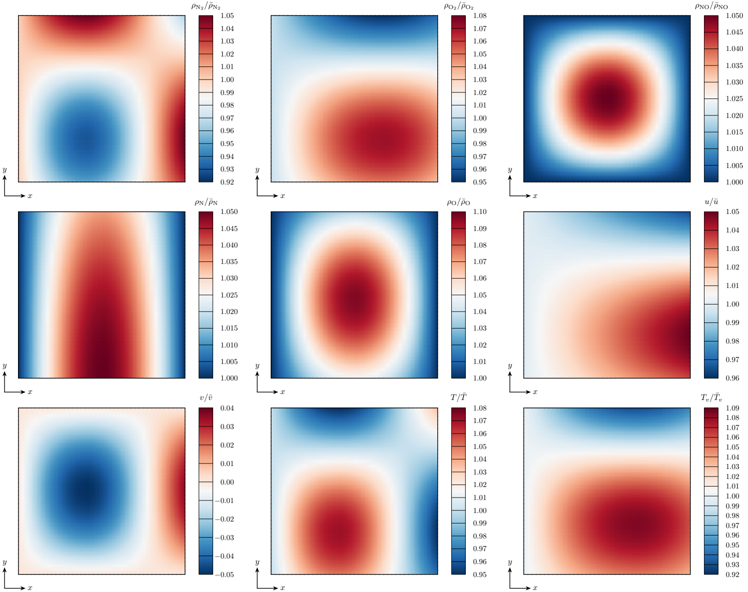

2D Supersonic Flow in Thermal Equilibrium using a Manufactured Solution

Variable	Value	Units
$\bar{\rho}_{N_2}$	0.77	kg/m^3
$\bar{\rho}_{O_2}$	0.20	kg/m^3
$\bar{\rho}_{NO}$	0.01	kg/m^3
$\bar{\rho}_{N}$	0.01	kg/m^3
$\bar{\rho}_{O}$	0.01	kg/m^3
$\bar{T}$	3500	K
$\bar{M}$	2.5	
ϵ	0.05	

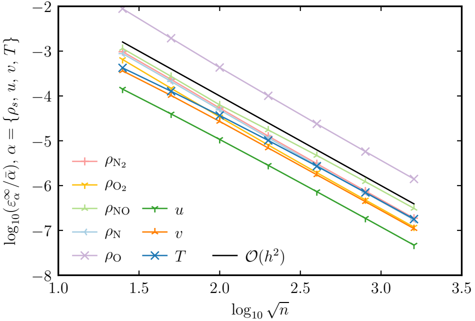

Mesh	ρ_{N_2}	ρ_{O_2}	ρ_{NO}	ρ_N	ρ_O	u	v	T
1–2	2.0608	2.1382	2.0698	2.0644	2.1885	1.8425	1.8289	1.7351
2–3	2.1161	2.1219	2.1127	2.1072	2.1697	1.8875	1.9220	1.7923
3–4	2.0798	2.0813	1.8555	2.0754	2.0971	1.9200	1.9686	1.8525
4–5	2.0456	2.0458	1.8917	2.0428	2.0806	1.9522	1.9871	1.9079
5–6	2.0243	2.0243	1.9427	2.0228	2.0529	1.9735	1.9939	1.9485
6–7	2.0125	2.0125	1.9790	2.0118	2.0318	1.9865	1.9969	1.9737

2D MMS, $n_s = 5$, $T_v = T$, $\dot{\mathbf{w}} \neq \mathbf{0}$: Observed accuracy p using L^∞-norms of the error

2D Hypersonic Flow in Thermal Nonequilibrium using a Manufactured Solution

Variable	Value	Units
$\bar{\rho}_{\mathrm{N}_2}$	0.0077	kg/m^3
$\bar{\rho}_{\mathrm{O}_2}$	0.0020	kg/m^3
$\bar{\rho}_{\mathrm{NO}}$	0.0001	kg/m^3
$\bar{\rho}_{\mathrm{N}}$	0.0001	kg/m^3
$\bar{\rho}_{\mathrm{O}}$	0.0001	kg/m^3
$\bar{T}$	5000	K
$\bar{T}_v$	1000	K
$\bar{M}$	8	
ϵ	0.05	

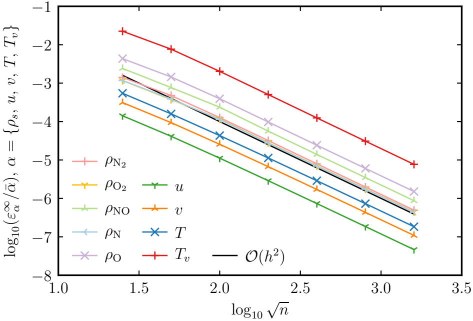

Mesh	ρ_{N_2}	ρ_{O_2}	ρ_{NO}	ρ_{N}	ρ_{O}	u	v	T	T_v
1–2	1.5659	1.6370	1.6555	1.6046	1.5869	1.7742	1.7337	1.7814	1.5545
2–3	1.9067	1.6944	1.6986	1.7598	1.8819	1.8916	1.8701	1.8768	1.9150
3–4	1.9868	2.0475	2.0698	2.0477	2.0110	1.9488	1.9357	1.9349	2.0082
4–5	2.0074	1.9941	2.0138	1.9936	2.0089	1.9752	1.9684	1.9672	2.0168
5–6	2.0062	1.9939	2.0004	1.9935	2.0061	1.9879	1.9843	1.9836	2.0111
6–7	2.0037	1.9965	1.9994	1.9962	1.9955	1.9940	1.9922	1.9918	2.0063

2D MMS, $n_s = 5$, $T_v \neq T$, $\dot{\mathbf{w}} \neq \mathbf{0}$: Observed accuracy p using L^∞-norms of the error

Outline

- Introduction
- Governing Equations
- Verification Techniques for Spatial Accuracy
- Spatial-Discretization Verification Results
- Verification Techniques for Thermochemical Source Term
  - Techniques
  - Distinctive Features
- Thermochemical-Source-Term Verification Results
- Summary

Verification Techniques for Thermochemical Source Term

- $\mathbf{S}(\mathbf{U}) = \left[\dot{\mathbf{w}};\, \mathbf{0};\, 0;\, Q_{t-v} + \mathbf{e}_v^T \dot{\mathbf{w}}\right]$ is algebraic

Verification Techniques for Thermochemical Source Term

- $\mathbf{S}\left(\mathbf{U}\right) = \left[\dot{\mathbf{w}};\, \mathbf{0};\, 0;\, Q_{t-v} + \mathbf{e}_v^T\dot{\mathbf{w}}\right]$ is algebraic
  - $\mathbf{S}\left(\mathbf{U}\right)$ computed by same code for both sides of $\mathbf{r}_h(\mathbf{U}_h) = \mathbf{r}(\mathbf{U}_{\mathrm{MS}})$

Verification Techniques for Thermochemical Source Term

- $\mathbf{S}(\mathbf{U}) = \left[\dot{\mathbf{w}};\, \mathbf{0};\, 0;\, Q_{t-v} + \mathbf{e}_v^T \dot{\mathbf{w}}\right]$ is algebraic
  - $\mathbf{S}(\mathbf{U})$ computed by same code for both sides of $\mathbf{r}_h(\mathbf{U}_h) = \mathbf{r}(\mathbf{U}_{\mathrm{MS}})$
  - Manufactured solutions will **not** detect implementation errors

Verification Techniques for Thermochemical Source Term

- $\mathbf{S}(\mathbf{U}) = \left[\dot{\mathbf{w}};\, \mathbf{0};\, 0;\, Q_{t-v} + \mathbf{e}_v^T \dot{\mathbf{w}}\right]$ is algebraic
  - $\mathbf{S}(\mathbf{U})$ computed by same code for both sides of $\mathbf{r}_h(\mathbf{U}_h) = \mathbf{r}(\mathbf{U}_{\mathrm{MS}})$
  - Manufactured solutions will **not** detect implementation errors
- Compute $Q_{t-v}(\boldsymbol{\rho}, T, T_v)$, $\mathbf{e}_v(\boldsymbol{\rho}, T, T_v)$, and $\dot{\mathbf{w}}(\boldsymbol{\rho}, T, T_v)$

Verification Techniques for Thermochemical Source Term

- $\mathbf{S}\left(\mathbf{U}\right) = \left[\dot{\mathbf{w}};\ \mathbf{0};\ 0;\ Q_{t-v} + \mathbf{e}_v^T\dot{\mathbf{w}}\right]$ is algebraic
  - $\mathbf{S}\left(\mathbf{U}\right)$ computed by same code for both sides of $\mathbf{r}_h(\mathbf{U}_h) = \mathbf{r}(\mathbf{U}_{\mathrm{MS}})$
  - Manufactured solutions will **not** detect implementation errors
- Compute $Q_{t-v}(\boldsymbol{\rho}, T, T_v)$, $\mathbf{e}_v(\boldsymbol{\rho}, T, T_v)$, and $\dot{\mathbf{w}}(\boldsymbol{\rho}, T, T_v)$
  - For single-cell mesh when initialized to $\{\boldsymbol{\rho},\ T,\ T_v\}$ with no velocity

Verification Techniques for Thermochemical Source Term

- $\mathbf{S}(\mathbf{U}) = \left[\dot{\mathbf{w}};\, \mathbf{0};\, 0;\, Q_{t-v} + \mathbf{e}_v^T \dot{\mathbf{w}}\right]$ is algebraic
  - $\mathbf{S}(\mathbf{U})$ computed by same code for both sides of $\mathbf{r}_h(\mathbf{U}_h) = \mathbf{r}(\mathbf{U}_{\mathrm{MS}})$
  - Manufactured solutions will **not** detect implementation errors
- Compute $Q_{t-v}(\boldsymbol{\rho}, T, T_v)$, $\mathbf{e}_v(\boldsymbol{\rho}, T, T_v)$, and $\dot{\mathbf{w}}(\boldsymbol{\rho}, T, T_v)$
  - For single-cell mesh when initialized to $\{\boldsymbol{\rho},\, T,\, T_v\}$ with no velocity
  - For many values of $\{\boldsymbol{\rho},\, T,\, T_v\}$

Verification Techniques for Thermochemical Source Term

- $\mathbf{S}(\mathbf{U}) = \left[\dot{\mathbf{w}};\, \mathbf{0};\, 0;\, Q_{t-v} + \mathbf{e}_v^T \dot{\mathbf{w}}\right]$ is algebraic
  - $\mathbf{S}(\mathbf{U})$ computed by same code for both sides of $\mathbf{r}_h(\mathbf{U}_h) = \mathbf{r}(\mathbf{U}_{\text{MS}})$
  - Manufactured solutions will **not** detect implementation errors

- Compute $Q_{t-v}(\boldsymbol{\rho}, T, T_v)$, $\mathbf{e}_v(\boldsymbol{\rho}, T, T_v)$, and $\dot{\mathbf{w}}(\boldsymbol{\rho}, T, T_v)$
  - For single-cell mesh when initialized to $\{\boldsymbol{\rho},\, T,\, T_v\}$ with no velocity
  - For many values of $\{\boldsymbol{\rho},\, T,\, T_v\}$
  - Compare with independently developed code

Verification Techniques for Thermochemical Source Term

- $\mathbf{S}(\mathbf{U}) = \left[\dot{\mathbf{w}};\, \mathbf{0};\, 0;\, Q_{t-v} + \mathbf{e}_v^T \dot{\mathbf{w}}\right]$ is algebraic
  - $\mathbf{S}(\mathbf{U})$ computed by same code for both sides of $\mathbf{r}_h(\mathbf{U}_h) = \mathbf{r}(\mathbf{U}_{\text{MS}})$
  - Manufactured solutions will **not** detect implementation errors

- Compute $Q_{t-v}(\boldsymbol{\rho}, T, T_v)$, $\mathbf{e}_v(\boldsymbol{\rho}, T, T_v)$, and $\dot{\mathbf{w}}(\boldsymbol{\rho}, T, T_v)$
  - For single-cell mesh when initialized to $\{\boldsymbol{\rho},\, T,\, T_v\}$ with no velocity
  - For many values of $\{\boldsymbol{\rho},\, T,\, T_v\}$
  - Compare with independently developed code
  - Perform convergence studies on distribution and difference

Verification Techniques for Thermochemical Source Term

- $\mathbf{S}(\mathbf{U}) = \left[\dot{\mathbf{w}};\, \mathbf{0};\, 0;\, Q_{t-v} + \mathbf{e}_v^T \dot{\mathbf{w}}\right]$ is algebraic
  - $\mathbf{S}(\mathbf{U})$ computed by same code for both sides of $\mathbf{r}_h(\mathbf{U}_h) = \mathbf{r}(\mathbf{U}_{\mathrm{MS}})$
  - Manufactured solutions will **not** detect implementation errors

- Compute $Q_{t-v}(\boldsymbol{\rho}, T, T_v)$, $\mathbf{e}_v(\boldsymbol{\rho}, T, T_v)$, and $\dot{\mathbf{w}}(\boldsymbol{\rho}, T, T_v)$
  - For single-cell mesh when initialized to $\{\boldsymbol{\rho},\, T,\, T_v\}$ with no velocity
  - For many values of $\{\boldsymbol{\rho},\, T,\, T_v\}$
  - Compare with independently developed code
  - Perform convergence studies on distribution and difference

- For each query, compute symmetric relative difference

$$\delta_\beta = 2\frac{|\beta_{\texttt{SPARC}} - \beta'|}{|\beta_{\texttt{SPARC}}| + |\beta'|}$$

$$\beta = \left\{Q_{t-v},\, e_{v_{\mathrm{N}_2}},\, e_{v_{\mathrm{O}_2}},\, e_{v_{\mathrm{NO}}},\, \dot{w}_{\mathrm{N}_2},\, \dot{w}_{\mathrm{O}_2},\, \dot{w}_{\mathrm{NO}},\, \dot{w}_{\mathrm{N}},\, \dot{w}_{\mathrm{O}}\right\}$$

Distinctive Features

This is **not** typical low-rigor code-to-code comparison

Distinctive Features

This is **not** typical low-rigor code-to-code comparison

Distinctive and rigorous features:

Distinctive Features

This is **not** typical low-rigor code-to-code comparison

Distinctive and rigorous features:

- Code is independently developed **internally**

Distinctive Features

This is **not** typical low-rigor code-to-code comparison

Distinctive and rigorous features:

- Code is independently developed **internally**
  - Uses **same** models and material properties expected from `SPARC`

Distinctive Features

This is **not** typical low-rigor code-to-code comparison

Distinctive and rigorous features:

- Code is independently developed **internally**
  - Uses **same** models and material properties expected from `SPARC`
  - Models and properties taken **directly** from the original references

Distinctive Features

This is **not** typical low-rigor code-to-code comparison

Distinctive and rigorous features:

- Code is independently developed **internally**
  - Uses **same** models and material properties expected from `SPARC`
  - Models and properties taken **directly** from the original references
  - With external software, assessing implementation is non-trivial

Distinctive Features

This is **not** typical low-rigor code-to-code comparison

Distinctive and rigorous features:

- Code is independently developed **internally**
  - Uses **same** models and material properties expected from `SPARC`
  - Models and properties taken **directly** from the original references
  - With external software, assessing implementation is non-trivial
    - Variety of models and properties complicates quantifying agreement

Distinctive Features

This is **not** typical low-rigor code-to-code comparison

Distinctive and rigorous features:

- Code is independently developed **internally**
  - Uses **same** models and material properties expected from `SPARC`
  - Models and properties taken **directly** from the original references
  - With external software, assessing implementation is non-trivial
    - Variety of models and properties complicates quantifying agreement
    - Less control over precision of output

Distinctive Features

This is **not** typical low-rigor code-to-code comparison

Distinctive and rigorous features:

- Code is independently developed **internally**
  - Uses **same** models and material properties expected from `SPARC`
  - Models and properties taken **directly** from the original references
  - With external software, assessing implementation is non-trivial
    - Variety of models and properties complicates quantifying agreement
    - Less control over precision of output
- Relative differences required to be **low** – near machine precision

Distinctive Features

This is **not** typical low-rigor code-to-code comparison

Distinctive and rigorous features:

- Code is independently developed **internally**
  - Uses **same** models and material properties expected from `SPARC`
  - Models and properties taken **directly** from the original references
  - With external software, assessing implementation is non-trivial
    - Variety of models and properties complicates quantifying agreement
    - Less control over precision of output
- Relative differences required to be **low** – near machine precision
  - Models and material properties are the same

Distinctive Features

This is **not** typical low-rigor code-to-code comparison

Distinctive and rigorous features:

- Code is independently developed **internally**
  - Uses **same** models and material properties expected from `SPARC`
  - Models and properties taken **directly** from the original references
  - With external software, assessing implementation is non-trivial
    - Variety of models and properties complicates quantifying agreement
    - Less control over precision of output
- Relative differences required to be **low** – near machine precision
  - Models and material properties are the same
  - Typically code-to-code comparison accepts a few percent

Distinctive Features

This is **not** typical low-rigor code-to-code comparison

Distinctive and rigorous features:

- Code is independently developed **internally**
  - Uses **same** models and material properties expected from `SPARC`
  - Models and properties taken **directly** from the original references
  - With external software, assessing implementation is non-trivial
    - Variety of models and properties complicates quantifying agreement
    - Less control over precision of output
- Relative differences required to be **low** – near machine precision
  - Models and material properties are the same
  - Typically code-to-code comparison accepts a few percent
- **Wide** condition coverage

Distinctive Features

This is **not** typical low-rigor code-to-code comparison

Distinctive and rigorous features:

- Code is independently developed **internally**
  - Uses **same** models and material properties expected from `SPARC`
  - Models and properties taken **directly** from the original references
  - With external software, assessing implementation is non-trivial
    - Variety of models and properties complicates quantifying agreement
    - Less control over precision of output
- Relative differences required to be **low** – near machine precision
  - Models and material properties are the same
  - Typically code-to-code comparison accepts a few percent
- **Wide** condition coverage
  - Comparison is queried for 1000s of conditions, spans extreme ranges

Distinctive Features

This is **not** typical low-rigor code-to-code comparison

Distinctive and rigorous features:

- Code is independently developed **internally**
  - Uses **same** models and material properties expected from `SPARC`
  - Models and properties taken **directly** from the original references
  - With external software, assessing implementation is non-trivial
    - Variety of models and properties complicates quantifying agreement
    - Less control over precision of output
- Relative differences required to be **low** – near machine precision
  - Models and material properties are the same
  - Typically code-to-code comparison accepts a few percent
- **Wide** condition coverage
  - Comparison is queried for 1000s of conditions, spans extreme ranges
  - Code-to-code comparison typically considers single or few conditions

Outline

- Introduction
- Governing Equations
- Verification Techniques for Spatial Accuracy
- Spatial-Discretization Verification Results
- Verification Techniques for Thermochemical Source Term
- Thermochemical-Source-Term Verification Results
  - Samples of $Q_{t-v}(\boldsymbol{\rho}, T, T_v)$, $\mathbf{e}_v(\boldsymbol{\rho}, T, T_v)$, and $\dot{\mathbf{w}}(\boldsymbol{\rho}, T, T_v)$
  - Nonzero Relative Differences in Q_{t-v} and $\mathbf{e}_v$
  - Nonzero Relative Differences in $\dot{\mathbf{w}}$
  - Convergence History of Relative Differences
- Summary

Convergence History of $Q_{t-v}(\boldsymbol{\rho}, T, T_v)$, $\mathbf{e}_v(\boldsymbol{\rho}, T, T_v)$, and $\dot{\mathbf{w}}(\boldsymbol{\rho}, T, T_v)$

Variable	Minimum	Maximum	Units	Spacing
ρ_{N_2}	10^{-6}	10^1	kg/m^3	Logarithmic
ρ_{O_2}	10^{-6}	10^1	kg/m^3	Logarithmic
ρ_{NO}	10^{-6}	10^1	kg/m^3	Logarithmic
ρ_{N}	10^{-6}	10^1	kg/m^3	Logarithmic
ρ_{O}	10^{-6}	10^1	kg/m^3	Logarithmic
T	100	15,000	K	Linear
T_v	100	15,000	K	Linear

Ranges and spacings for Latin hypercube samples

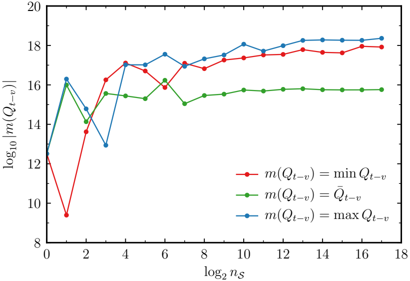

Minimum, mean, and maximum

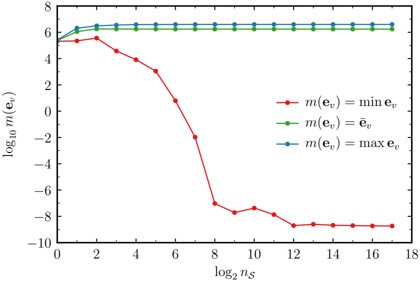

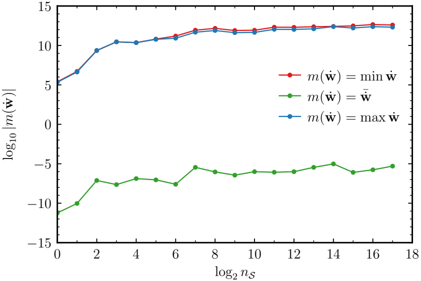

Distributions of $Q_{t-v}(\boldsymbol{\rho}, T, T_v)$, $\mathbf{e}_v(\boldsymbol{\rho}, T, T_v)$, and $\dot{\mathbf{w}}(\boldsymbol{\rho}, T, T_v)$

Variable	Minimum	Maximum	Units	Spacing
ρ_{N_2}	10^{-6}	10^{1}	$\mathrm{kg/m^3}$	Logarithmic
ρ_{O_2}	10^{-6}	10^{1}	$\mathrm{kg/m^3}$	Logarithmic
ρ_{NO}	10^{-6}	10^{1}	$\mathrm{kg/m^3}$	Logarithmic
ρ_{N}	10^{-6}	10^{1}	$\mathrm{kg/m^3}$	Logarithmic
ρ_{O}	10^{-6}	10^{1}	$\mathrm{kg/m^3}$	Logarithmic
T	100	15,000	K	Linear
T_v	100	15,000	K	Linear

Ranges and spacings for Latin hypercube samples

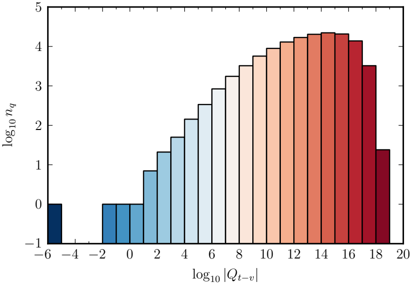

Distribution of absolute values for $n_{\mathcal{S}} = 2^{17} = 131,072$

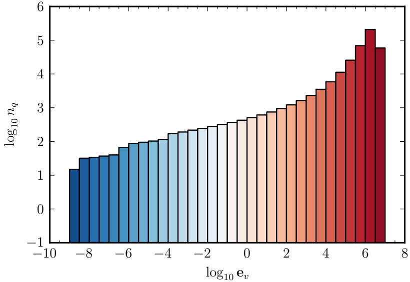

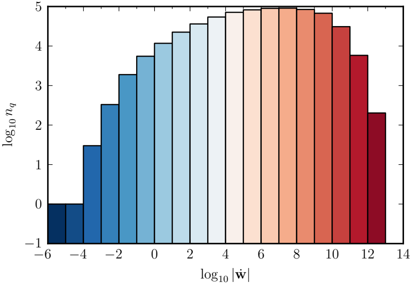

Original Nonzero Relative Differences in Q_{t-v} and $\mathbf{e}_v$

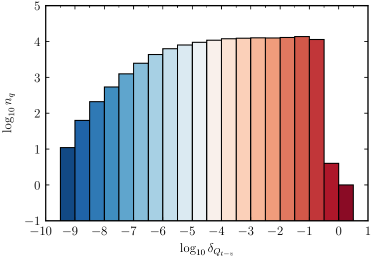

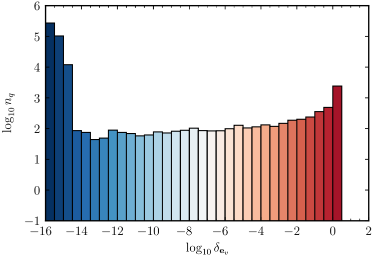

Original Nonzero Relative Differences in Q_{t-v} and $\mathbf{e}_v$

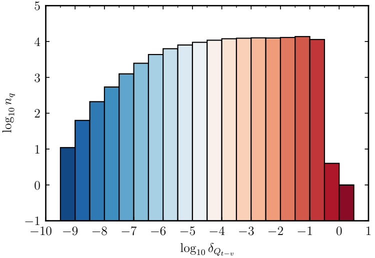

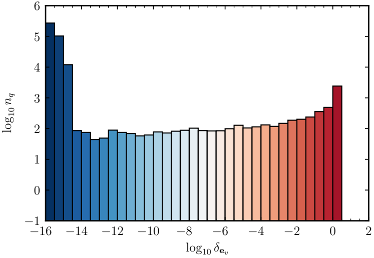

- Relative differences are not near machine precision

Original Nonzero Relative Differences in Q_{t-v} and $\mathbf{e}_v$

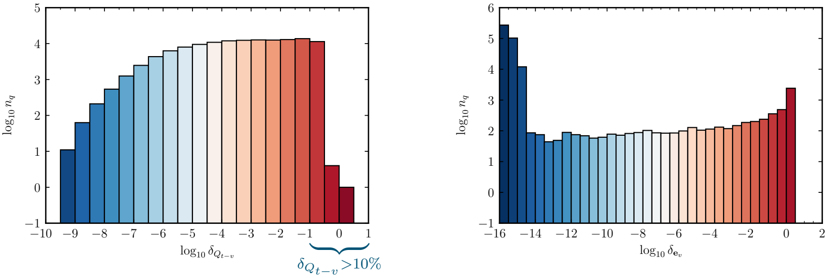

- Relative differences are not near machine precision
- $\delta_{Q_{t-v}} > 10\%$ in 8.7% of simulations

Original Nonzero Relative Differences in Q_{t-v} and $\mathbf{e}_v$

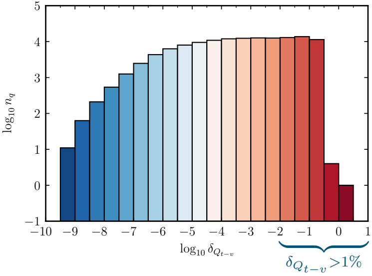

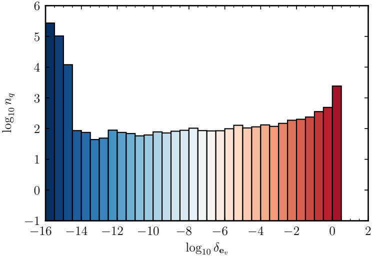

- Relative differences are not near machine precision
- $\delta_{Q_{t-v}} > 10\%$ in 8.7% of simulations
- $\delta_{Q_{t-v}} > 1\%$ in 29% of simulations

Original Nonzero Relative Differences in Q_{t-v} and $\mathbf{e}_v$

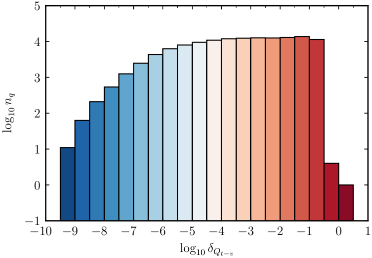

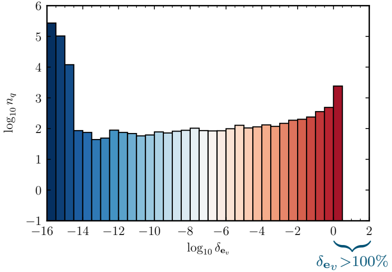

- Relative differences are not near machine precision
- $\delta_{Q_{t-v}} > 10\%$ in 8.7% of simulations
- $\delta_{Q_{t-v}} > 1\%$ in 29% of simulations
- $\delta_{\mathbf{e}_v} > 100\%$ for some simulations

Causes of Large Relative Differences in Q_{t-v} and $\mathbf{e}_v$

Two causes:

Causes of Large Relative Differences in Q_{t-v} and $\mathbf{e}_v$

Two causes:

- **Incorrect lookup table values** for vibrational constants
  - For N_2 and O_2 when the colliding species is NO
  - Introduced error in Q_{t-v} for all simulations
  - For high-enthalpy (20 MJ/kg), hypersonic, laminar double-cone flow, 1.4% change in pressure and 2.7% change in heat flux

Causes of Large Relative Differences in Q_{t-v} and $\mathbf{e}_v$

Two causes:

- **Incorrect lookup table values** for vibrational constants
  - For N_2 and O_2 when the colliding species is NO
  - Introduced error in Q_{t-v} for all simulations
  - For high-enthalpy (20 MJ/kg), hypersonic, laminar double-cone flow, 1.4% change in pressure and 2.7% change in heat flux
- **Loose convergence criteria** for computing T_v from ρe_v
  - Unsuitable for low values of T_v
  - Introduced errors in Q_{t-v}, $\mathbf{e}_v$, and $\dot{\mathbf{w}}$ for a few simulations
  - For converged, steady problem, original criteria are acceptable

Corrected Nonzero Relative Differences in Q_{t-v} and $\mathbf{e}_v$

Original lookup table and convergence criteria

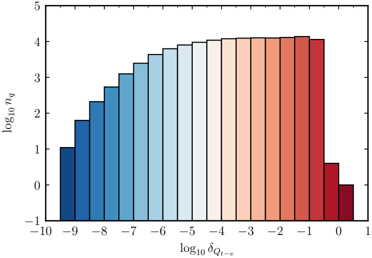

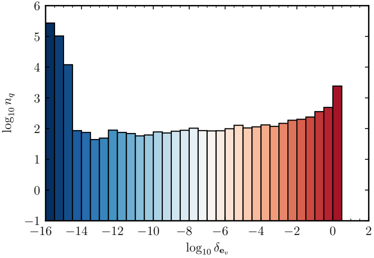

Corrected Nonzero Relative Differences in Q_{t-v} and $\mathbf{e}_v$

Original lookup table and convergence criteria

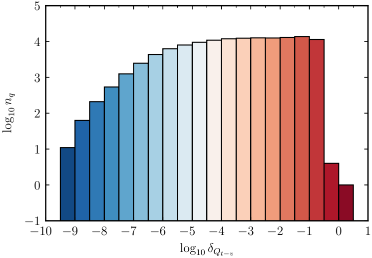

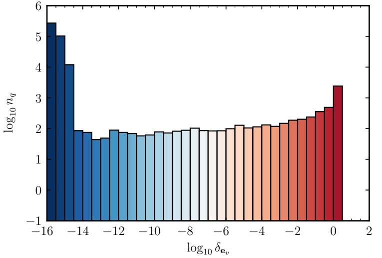

Corrected lookup table and tighter convergence criteria

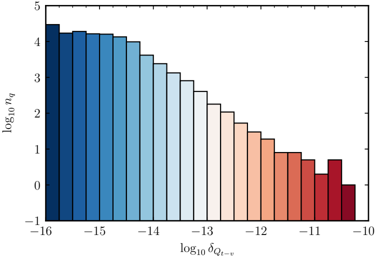

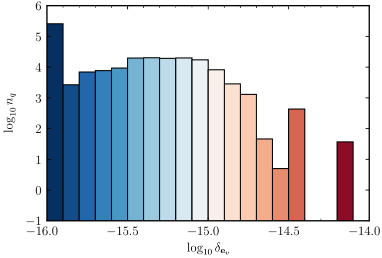

Corrected Nonzero Relative Differences in Q_{t-v} and $\mathbf{e}_v$

- Relative differences are consistent with our expectations

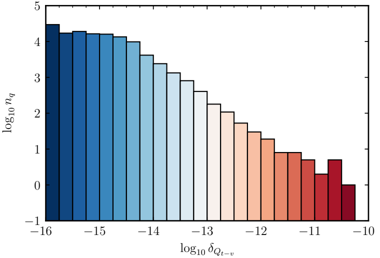

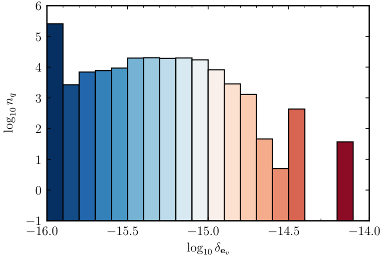

Corrected Nonzero Relative Differences in Q_{t-v} and $\mathbf{e}_v$

- Relative differences are consistent with our expectations
- $\delta_{Q_{t-v}} < 10^{-10}$ and $\delta_{\mathbf{e}_v} < 10^{-14}$ in all simulations

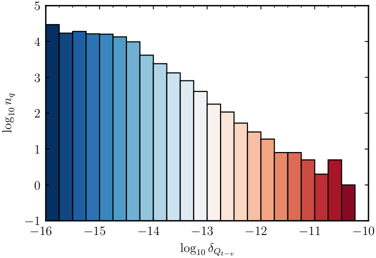

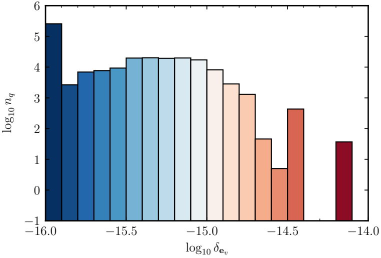

Corrected Nonzero Relative Differences in Q_{t-v} and $\mathbf{e}_v$

- Relative differences are consistent with our expectations
- $\delta_{Q_{t-v}} < 10^{-10}$ and $\delta_{\mathbf{e}_v} < 10^{-14}$ in all simulations
- $\delta_{Q_{t-v}} > 10^{-12}$ in 48/131,072 simulations

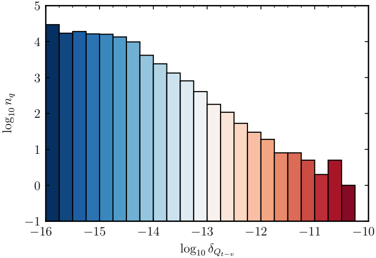

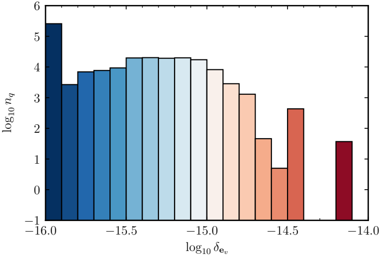

Corrected Nonzero Relative Differences in Q_{t-v} and $\mathbf{e}_v$

- Relative differences are consistent with our expectations
- $\delta_{Q_{t-v}} < 10^{-10}$ and $\delta_{\mathbf{e}_v} < 10^{-14}$ in all simulations
- $\delta_{Q_{t-v}} > 10^{-12}$ in 48/131,072 simulations
  - T and T_v have relative difference less than 0.2%

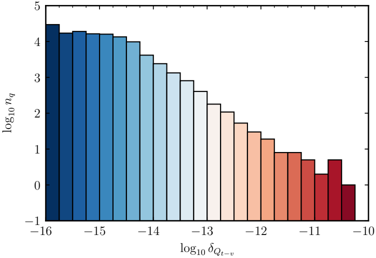

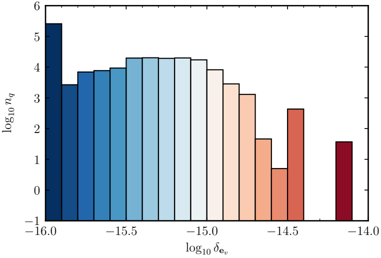

Corrected Nonzero Relative Differences in Q_{t-v} and $\mathbf{e}_v$

- Relative differences are consistent with our expectations
- $\delta_{Q_{t-v}} < 10^{-10}$ and $\delta_{\mathbf{e}_v} < 10^{-14}$ in all simulations
- $\delta_{Q_{t-v}} > 10^{-12}$ in 48/131,072 simulations
  - T and T_v have relative difference less than 0.2%
  - In numerator of $\frac{e_{v_{s,m}}(T) - e_{v_{s,m}}(T_v)}{\langle \tau_{s,m} \rangle}$, $e_{v_{s,m}}(T)$ and $e_{v_{s,m}}(T_v)$ share many leading digits

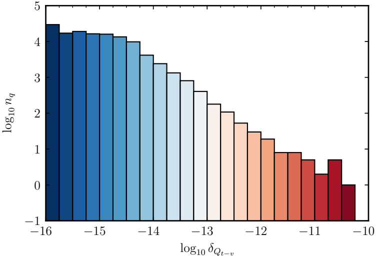

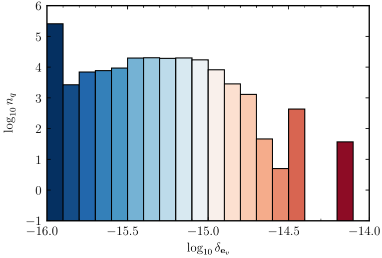

Corrected Nonzero Relative Differences in Q_{t-v} and $\mathbf{e}_v$

- Relative differences are consistent with our expectations
- $\delta_{Q_{t-v}} < 10^{-10}$ and $\delta_{\mathbf{e}_v} < 10^{-14}$ in all simulations
- $\delta_{Q_{t-v}} > 10^{-12}$ in 48/131,072 simulations
  - T and T_v have relative difference less than 0.2%
  - In numerator of $\frac{e_{v_{s,m}}(T)-e_{v_{s,m}}(T_v)}{\langle\tau_{s,m}\rangle}$, $e_{v_{s,m}}(T)$ and $e_{v_{s,m}}(T_v)$ share many leading digits
  - Precision lost when computing difference

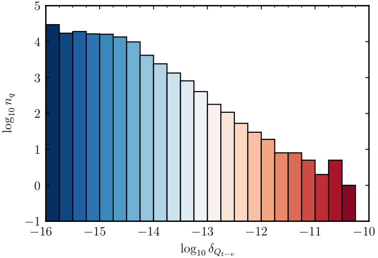

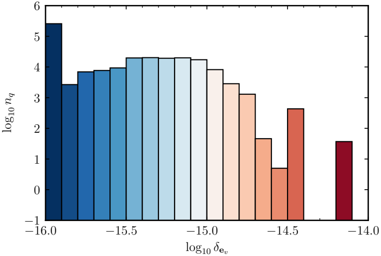

Nonzero Relative Differences in $\dot{\mathbf{w}}$

Original convergence criteria

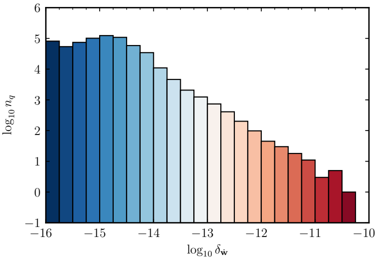

Tighter convergence criteria

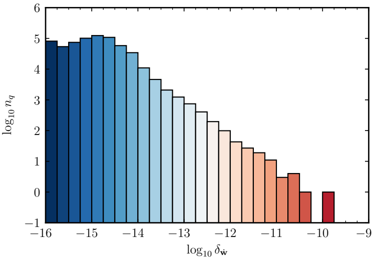

Nonzero Relative Differences in $\dot{\mathbf{w}}$

Original convergence criteria

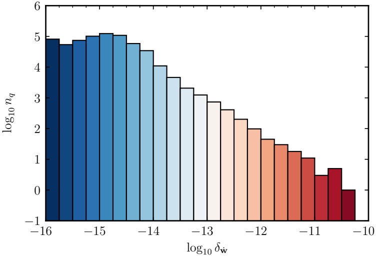

Tighter convergence criteria

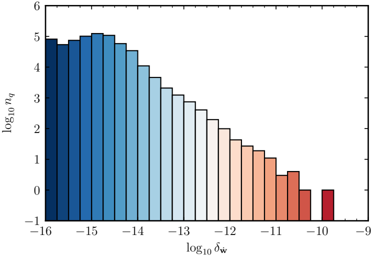

- Relative differences are consistent with our expectations

Nonzero Relative Differences in $\dot{\mathbf{w}}$

Original convergence criteria

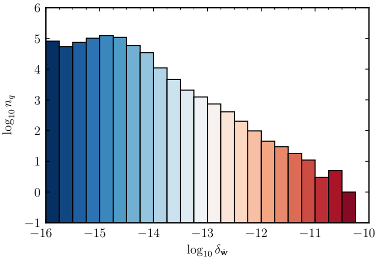

Tighter convergence criteria

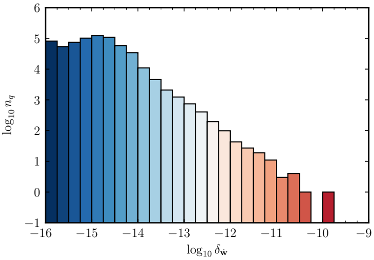

- Relative differences are consistent with our expectations
- $\delta_{\dot{\mathbf{w}}} < 10^{-9}$ in all simulations

Nonzero Relative Differences in $\dot{\mathbf{w}}$

Original convergence criteria

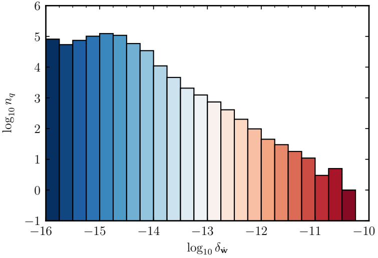

Tighter convergence criteria

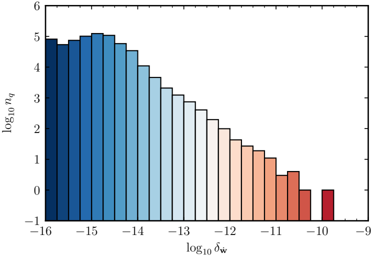

- Relative differences are consistent with our expectations
- $\delta_{\dot{\mathbf{w}}} < 10^{-9}$ in all simulations
- $\delta_{\dot{\mathbf{w}}} > 10^{-12}$ for 109/655,360 computed values (5 species, 131,072 simulations)

Nonzero Relative Differences in $\dot{\mathbf{w}}$

Original convergence criteria

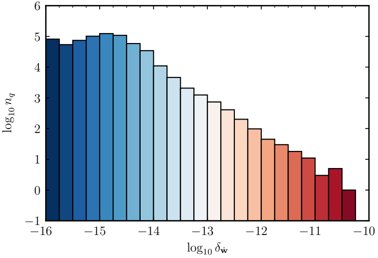

Tighter convergence criteria

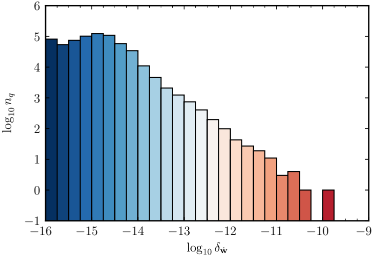

- Relative differences are consistent with our expectations
- $\delta_{\dot{\mathbf{w}}} < 10^{-9}$ in all simulations
- $\delta_{\dot{\mathbf{w}}} > 10^{-12}$ for 109/655,360 computed values (5 species, 131,072 simulations)
  - Due to precision loss that can occur from subtraction in $\dot{w}_s = M_s \sum_{r=1}^{n_r} (\beta_{s,r} - \alpha_{s,r}) (R_{f_r} - R_{b_r})$

Maximum Differences in $Q_{t-v}(\boldsymbol{\rho}, T, T_v)$, $\mathbf{e}_v(\boldsymbol{\rho}, T, T_v)$, and $\dot{\mathbf{w}}(\boldsymbol{\rho}, T, T_v)$

Variable	Minimum	Maximum	Units	Spacing
ρ_{N_2}	10^{-6}	10^1	kg/m^3	Logarithmic
ρ_{O_2}	10^{-6}	10^1	kg/m^3	Logarithmic
ρ_{NO}	10^{-6}	10^1	kg/m^3	Logarithmic
ρ_{N}	10^{-6}	10^1	kg/m^3	Logarithmic
ρ_{O}	10^{-6}	10^1	kg/m^3	Logarithmic
T	100	15,000	K	Linear
T_v	100	15,000	K	Linear

Ranges and spacings for Latin hypercube samples

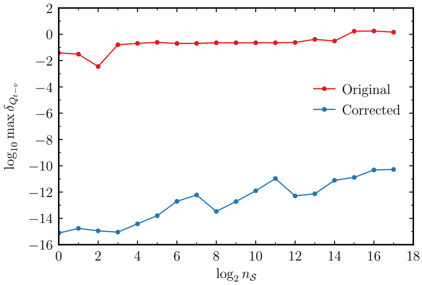

Maximum relative differences

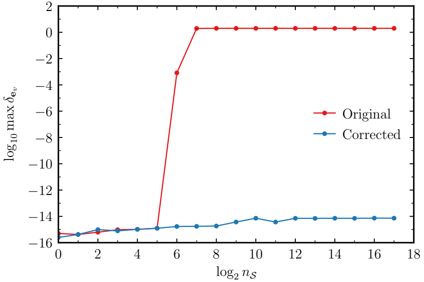

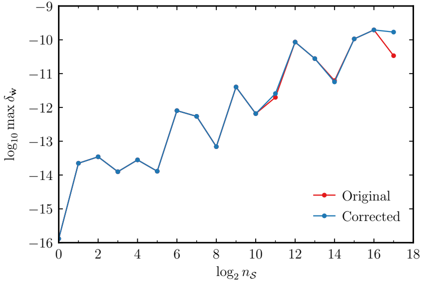

Outline

- Introduction
- Governing Equations
- Verification Techniques for Spatial Accuracy
- Spatial-Discretization Verification Results
- Verification Techniques for Thermochemical Source Term
- Thermochemical-Source-Term Verification Results
- Summary
  - Code-Verification Techniques

Code-Verification Techniques

- Manufactured and exact solutions
  - Effective approaches for verifying spatial accuracy – detected multiple issues
  - Rigorous norms improve effectiveness – L^∞-norm of error more useful
  - Insufficient for algebraic source terms – both evaluations the same
- Thermochemical-source-term approach
  - Effective approach for verifying implementation – detected multiple issues
  - Convergence study important to determine whether samples sufficiently span ranges

Additional Information

B. Freno, B. Carnes, V. Weirs
Code-Verification techniques for hypersonic reacting flows in thermochemical nonequilibrium
Journal of Computational Physics (2021) arXiv:2007.14376

Questions?

Sandia National Laboratories is a multimission laboratory managed and operated by National Technology & Engineering Solutions of Sandia, LLC, a wholly owned subsidiary of Honeywell International Inc., for the U.S. Department of Energy's National Nuclear Security Administration under contract DE-NA0003525.